

Accepted Manuscript

Towards a characterization of the structural determinants of specificity in the macrocyclizing thioesterase for deoxyerythronolide B biosynthesis

Panos Argyropoulos, Fabien Bergeret, Christophe Pardin, Janice M. Reimer, Atahualpa Pinto, Christopher N. Boddy, T. Martin Schmeing

PII: S0304-4165(15)00324-4
DOI: doi: [10.1016/j.bbagen.2015.11.007](https://doi.org/10.1016/j.bbagen.2015.11.007)
Reference: BBAGEN 28330

To appear in: *BBA - General Subjects*

Received date: 21 August 2015
Revised date: 13 November 2015
Accepted date: 20 November 2015



Please cite this article as: Panos Argyropoulos, Fabien Bergeret, Christophe Pardin, Janice M. Reimer, Atahualpa Pinto, Christopher N. Boddy, T. Martin Schmeing, Towards a characterization of the structural determinants of specificity in the macrocyclizing thioesterase for deoxyerythronolide B biosynthesis, *BBA - General Subjects* (2015), doi: [10.1016/j.bbagen.2015.11.007](https://doi.org/10.1016/j.bbagen.2015.11.007)

This is a PDF file of an unedited manuscript that has been accepted for publication. As a service to our customers we are providing this early version of the manuscript. The manuscript will undergo copyediting, typesetting, and review of the resulting proof before it is published in its final form. Please note that during the production process errors may be discovered which could affect the content, and all legal disclaimers that apply to the journal pertain.

**Towards a characterization of the structural determinants of specificity
in the macrocyclizing thioesterase for deoxyerythronolide B
biosynthesis**

Panos Argyropoulos,^{a†} Fabien Bergeret,^{b†} Christophe Pardin,^a Janice M. Reimer,^b
Atahualpa Pinto,^a Christopher N. Boddy^{a*} and T. Martin Schmeing,^{b**}

^aDepartment of Chemistry and Biomolecular Sciences, Centre for Catalysis Research and
Innovation, University of Ottawa, Ottawa, ON K1N 6N5, Canada

^bDepartment of Biochemistry, McGill University, Montréal, QC H3G 0B1, Canada
Groupe de Recherche Axé sur la Structure des Protéines (GRASP), McGill University,
Montréal, QC H3G 0B1, Canada

†These authors contributed equally to the work.

* Corresponding author. Tel.: 613-762-8900; fax: 613-562-5170.

** Corresponding author. Tel.: 514-398-2331; fax: 514-398-2983.

Email addresses: cboddy@uottawa.ca (C.N. B.) martin.schmeing@mcgill.ca (T. M. S.)

Key Words

Thioesterase, polyketide synthase, non-hydrolyzable acyl-enzyme intermediates, inhibition, high-resolution structure

Highlights

- 1.7 Å resolution structure of a new construct of the erythromycin thioesterase
- diphenyl phosphonate inhibitors of the erythromycin thioesterases were synthesized and assayed
- 2.1 Å resolution structure of allylphosphonate adduct of the erythromycin thioesterase
- Slow maturation of initial phosphonate-enzyme adduct limits use of diphenyl phosphonates esters

Abstract

Type I polyketide synthases (PKSs) are giant multidomain proteins that synthesize many therapeutics and other natural products. The synthesis proceeds by a thiotemplate mechanism whereby intermediates are covalently attached to the PKS. Release of the final polyketide is catalyzed by the terminal thioesterase (TE) domain through hydrolysis, transesterification, or macrocyclization. The PKS 6-deoxyerythronolide B synthase (DEBS) produces the 14-membered macrolide core of the clinically important antibiotic erythromycin. The TE domain of DEBS (DEBS TE) has well-established, empirically-defined specificities for hydrolysis or macrocyclization of native and modified substrates. We present efforts towards understanding the structural basis for the specificity of the thioesterase reaction in DEBS TE using a set of novel diphenyl alkylphosphonates, which mimic substrates that are specifically cyclized or hydrolyzed by DEBS TE. We have

determined structures of a new construct of DEBS TE alone at 1.7 Å, and DEBS TE bound with a simple allylphosphonate at 2.1 Å resolution. Other, more complex diphenyl alkylphosphonates inhibit DEBS TE, but we were unable to visualize these faithful cyclization analogs in complex with DEBS TE. This work represents a first step towards using DEBS TE complexed with sophisticated substrate analogues to decipher the specificity determinants in this important reaction.

Introduction

Type I polyketide synthases (PKSs) are giant multimodular proteins found in bacteria and fungi that synthesize secondary metabolites.[1,2] These polyketides play a crucial role in the fitness of microorganisms in their environment, impacting growth, colonization,[3] survival, and virulence.[4,5] Because of their highly selective and potent binding to specific biological targets, polyketides have been exploited as pharmaceuticals, including clinical antibiotics (erythromycin) anticancer agents (ixabepilone) and immunosuppressants (rapamycin).[2,6]

Type I PKSs synthesize polyketides from acyl-CoA building block substrates, using thio-templated logic, where intermediates are covalently shuttled between active sites attached to the phosphopantetheine arm of an acyl carrier protein (ACP) domain. Synthesis occurs in three stages, a loading stage, an elongation-modification stage, and an off-loading stage.[2] The most common off-loading mechanism in type I PKS biosynthesis is catalyzed by the thioesterase (TE) domain.[2,7,8] The TE domain uses a two-step mechanism (Figure 1). In the first step, the polyketide chain, which is linked by a thioester to the ACP, is transferred to the active site Ser of the catalytic Ser-His-Asp triad[8,9] of the TE through nucleophilic attack. The second step cleaves the acyl-TE intermediate, either by an intermolecular attack of an exogenous nucleophile (hydrolysis or transesterification) or an intramolecular attack by an internal nucleophile (macrolactamization, macrolactonization, or Claisen-like condensation), to release the completed polyketide from the PKS.

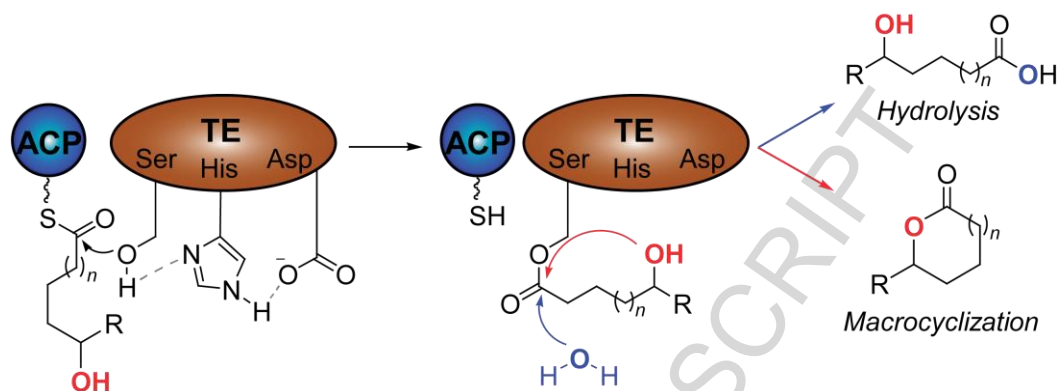


Figure 1. Thioesterases, which are serine hydrolases and possess the typical Ser-His-Asp serine hydrolase catalytic triad, play a key role in off-loading completed polyketide chains from the acyl carrier proteins of their biosynthetic pathways. This is catalyzed via a two-step mechanism. In the first step the completed polyketide chain is transferred to the active site Ser to make covalent complex between the TE and the polyketide chain. In the second step, nucleophilic attack on the activated ester bond of the acyl-enzyme intermediate leads to release of the polyketide. This can occur through either intramolecular nucleophilic attack, giving a macrocycle (arrow in red) or attack by water (arrow in blue) releasing the free acid. The mechanism controlling partitioning between macrocyclization and hydrolysis is uncharacterized.

Although the loading step typically has low substrate selectivity,[10] the release step is often highly selective. The best-characterized TE is from the 6-deoxyerythronolide B synthase (DEBS TE) (Figure S1). DEBS TE shows high stereo-, regio-, and chemo-selectivity in the release step. *In vivo*, it is able to cyclize a number of truncated or elongated erythronolide analogs forming 6, 8, 12, 14 or 16-membered rings.[11–14] *In vitro*, both the absolute stereochemistry of the nucleophilic alcohol and the presence of a carbonyl in the polyketide backbone are essential for cyclization.[15–18]

Structures of DEBS TE in the absence of ligands[19,20] gave high-resolution views of this important enzyme. Accompanying docking studies were used to suggest that H-bonding played a key role in controlling selectivity.[19] However, experimental testing of

this model called the conclusion into doubt.[21] The related TE domain from the pikromycin biosynthetic pathway (Pik-TE) has been determined in complex with non-hydrolyzable acyl analogs derived from diphenyl phosphonate esters.[22,23] The structures suggested that hydrophobic packing was a key mediator of enzyme-substrate interactions. However, the non-hydrolyzable acyl-enzyme intermediates used in the study had limited similarity to substrates known to undergo macrocyclization, thus tempering the use of these models for identifying discrete enzyme-substrate interactions that control the off-loading step. Ultimately, it is not yet possible to predict whether a particular substrate will undergo macrocyclization or hydrolysis.[10,17] Predicting and controlling the mode of release would be very useful for bioengineering experiments.

Here we present efforts towards characterizing the structural determinants of specificity of DEBS TE. We have designed a set of substituted diphenyl phosphonates that mimic substrates known to be cyclized or hydrolyzed by DEBS TE. These phosphonates covalently modify the active site Ser of DEBS TE and inhibit its function. We have designed and produced a modified construct of DEBS TE that is fully active and susceptible to inhibition by diphenyl phosphonates. We determined the structure of this novel DEBS TE construct at higher resolution (1.7 Å) than those previously available and also present a high-resolution structure of DEBS TE covalently modified with an allylphosphonate. Finally, we describe the challenges associated with producing non-hydrolyzable acyl-enzyme intermediates from complex phosphonates for use in understanding the selectivity of DEBS TE for macrocyclization versus hydrolysis activity.

Results and Discussion

Acyl- and peptidylphosphonates are a class of inhibitors that have been widely used to form a stable tetrahedral intermediate of serine proteases and TEs.[22–25] The successful use of diphenyl phosphonates in obtaining high-resolution acyl-enzyme intermediate structural data with the Pik TE,[22,23] suggested that these reagents would be applicable to the characterization of the enzyme-substrate interactions that govern substrate selectivity in DEBS TE. It should be possible to decipher the molecular basis for intramolecular cyclization by DEBS TE using phosphonate molecules that are highly analogous to DEBS TE substrates known to undergo either cyclization or macrocyclization.[17]

A new construct of the TE domain of DEBS

Our initial goal was thus to obtain a higher resolution structure of DEBS TE than previously published.[19,20] The Khosla and Stroud groups obtained two crystal structures for the DEBS TE, herein designated by their protein data base (PDB) codes, TE_{1KEZ} at 2.8 Å (PDB ID: 1KEZ) and TE_{1MO2} at 3.0 Å resolution (PDB ID: 1MO2). The N- and C-termini of these two structures were disordered, potentially disturbing the crystal packing and limiting the quality of diffraction pattern. Based on this observation, we truncated the N- and C-termini of DEBS TE, to generate a new construct containing residues S15 to S283 (TE₁₅₋₂₈₃) (Figure S2). This TE construct was overexpressed in *Escherichia coli* BL21(DE3) and purified to homogeneity by liquid chromatography with a high yield of 50 mg protein per liter of culture. This construct is robust and hydrolyzes

the N-acetyl cysteamine thioester of 3-hydroxyheptanoate with a rate ($V/[E]_t$) of 0.25 min^{-1} (Figure 2.), maintaining the same activity as the existing DEBS TE construct, which has turnover numbers between $0.1 - 0.8 \text{ min}^{-1}$ for a wide variety of substrates [15, 17, 21]. In addition, the enzyme could be stored at 37°C for 2 months without becoming inactive (data not shown).

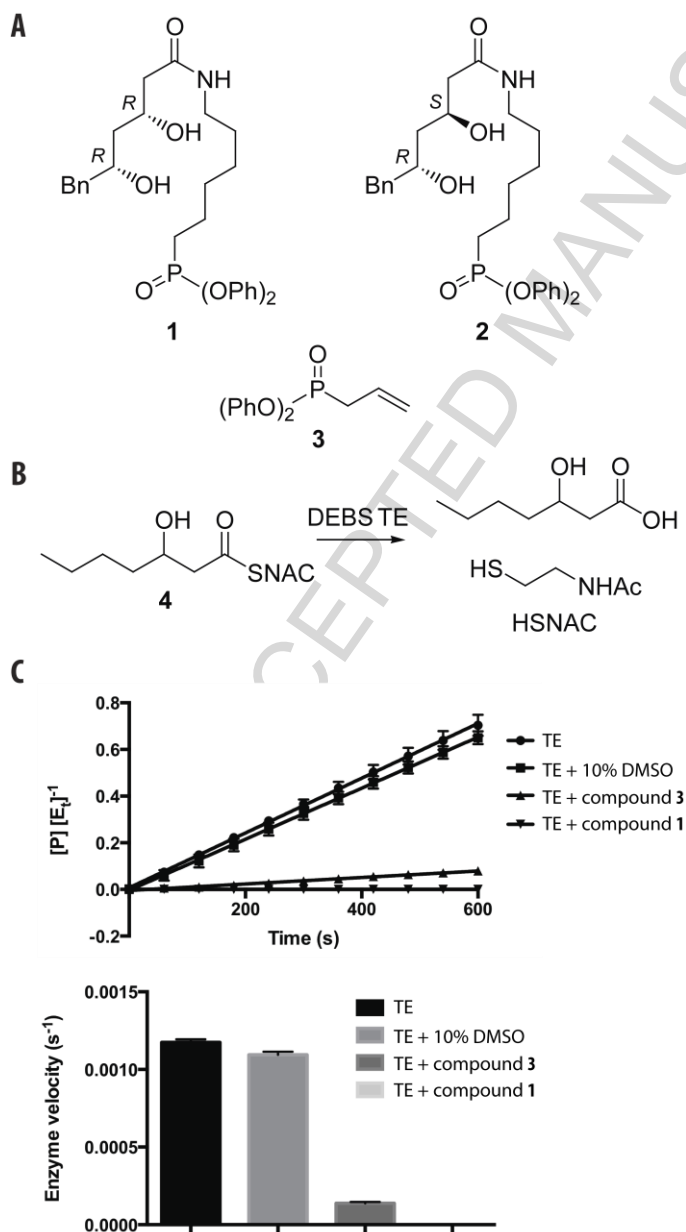


Figure 2. Inhibitors, model substrate and activity of DEBS TE. Panel A displays the chemical structures of the diphenyl phosphonates (1-3) used in this study. Panel B shows

the activity assay used to test the TE domains. Substrate (**4**) is hydrolyzed by DEBS TE releasing the free acid and N-acetylcysteamine (HSNAC). Panel C presents the normalized velocity of TE mediated hydrolysis of **4** under the listed conditions.

We attempted to reproduce the crystallization reported by the Khosla and Stroud groups,[19,20] but the crystals we obtained in these conditions with TE₁₅₋₂₈₃ did not diffract well. Therefore, we performed sparse matrix crystallization screening using sitting-drop vapour diffusion and obtained several new growth conditions producing large monocrystals. The best conditions were optimized to a precipitant solution of 0.1M Na-cacodylate pH=6.5, 35-38% PEG-300 and 0.18-0.24M Ca-acetate. These crystals belonged to space group P 3 2 1, and were phased using molecular replacement with TE_{1KEZ} as the search model. There is one molecule per asymmetric unit, all residues are visible in the electron density map, and the model has been refined to an R_{factor} of 15.6% and an R_{free} of 18.6% at 1.7 Å (Table 1) (PDB ID: 5D3K). These crystals are robust and reproducible, and the increased resolution obtained made them ideal for structural analysis of DEBS TE in complex with substrate analogues.

Overview of the structure of TE

DEBS TE₁₅₋₂₈₃ adopts the classic TE α/β hydrolase fold and has the catalytic triad of Ser-142, Asp-169 and His-259 (Figure 3) located in the middle of a long substrate channel, as previously reported.[20] Although TE₁₅₋₂₈₃ is overall quite similar to TE_{1KEZ} and TE_{1MO2}(C α -RMSD of 1.2 Å and 2.4 Å, respectively), there are some conformational differences between the three structures in two neighbouring, functionally important areas.

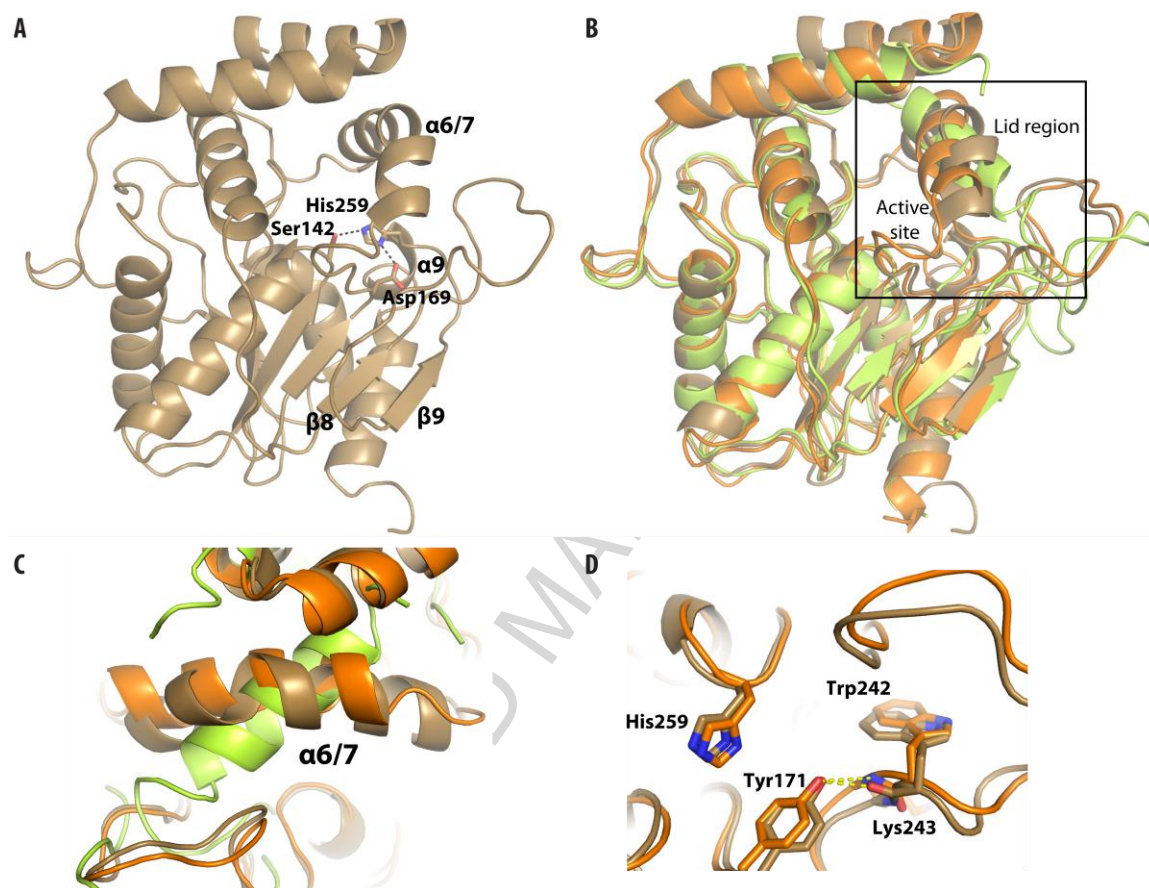


Figure 3. The structure of TE₁₅₋₂₈₃ in comparison to TE_{1KEZ} and TE_{1MO2}. Panel A shows TE₁₅₋₂₈₃ (brown) in cartoon representation with the catalytic residues in sticks. Panel B shows that the overall conformation is very similar to TE_{1KEZ} (orange) and TE_{1MO2} (green). Panel C shows that there is a substantial difference in conformation of the lid element. Panel D shows that at the active site Tyr₁₇₁ hydrogen bonds to the carbonyl of Trp₂₄₂, rather than to the amide of Lys₂₄₃.

The lid region is a mobile area known to interact with TE domain substrates, and is usually designated as α -helices 6 and 7 in TE domains. In DEBS TE the lid is between residues 176 to 193, and is a single α -helix between residues 178 and 190 (α -helix 6/7). The orientation of α -helix 6/7 differs between the three structures, and in TE₁₅₋₂₈₃ it is longer (residues 176-193) and kinked by ~ 65 degrees (Figure 3C). pH has been proposed to cause this difference in orientation, as repulsive interactions between residues that

become charged would result in changes to the size and the shape of the substrate channel.[20] The lid in TE₁₅₋₂₈₃ structure (determined at pH 6.5) forms a long and closed substrate channel, similar to TE_{1KEZ} (pH 7.2), while at more basic pH, the substrate channel is short and open (TE_{1MO2}, pH 8.5).

The active site His₂₅₉ is in a loop (residues 256-260) N-terminal to α -helix 9, and nearby to the long loop (residues 230-251) between β -strands 8 and 9. A hydrogen bond between the hydroxyl of Tyr₁₇₁ and the backbone amide of Lys₂₄₃, reported with TE_{1KEZ}, was suggested to be important for forming the active site and placing His₂₅₉ in the correct orientation for catalysis.[21] At higher pH (TE_{1MO2}, pH 8.5), or in the absence of this hydroxyl (Y172F mutant), the interaction is lost and His₂₅₉ is no longer positioned correctly for catalysis. Accordingly, in TE_{1MO2}, the conformation of residues 232-245 is completely altered and displaced by the lid, α -helix 9 unravels, and the loop with His₂₅₉ is splayed away from the active site. TE₁₅₋₂₈₃ shows an intact active site similar to TE_{1KEZ}. The interaction we observe, however, is the donation of a hydrogen bond from the hydroxyl of Tyr₁₇₁ to the backbone carbonyl of Trp₂₄₂, rather than the acceptance of one from the backbone amide of Lys₂₄₃ (Figure 3C). It is unclear whether the difference from 1KEZ is because the new maps allow better placement of residues 242 and 243, or if this represents a novel conformation.

Novel simple phosphonates inhibit DEBS TE activity

To validate the use of diphenyl phosphonates in producing a non-hydrolyzable acyl-enzyme intermediate with DEBS TE, we synthesized a number of simple diphenyl

phosphonates. Five different phosphonates were constructed using two different synthetic approaches: a Grignard or alkyl lithium type addition strategy and an S_N2 type strategy (Figure 4). All phosphonates were obtained at high purity and acceptable yields.

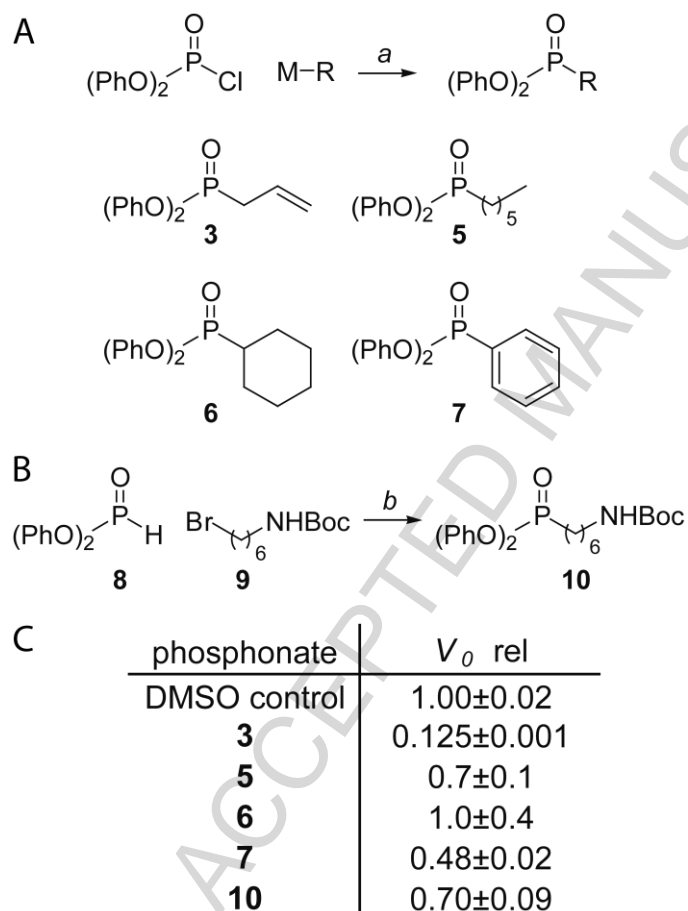


Figure 4. Synthesis of simple diphenyl phosphonates. Panel A shows the general scheme for the synthesis of simple diphenyl phosphonates via nucleophilic addition to diphenyl phosphoryl chloride. The four substrates accessed via this approach (**3**, **5-7**) are shown. *a*) diphenyl phosphoryl chloride, M-R, ether -78 °C, 3h, 8-24 %. Panel B shows the synthesis of the simple phosphonate **10** via nucleophilic attack by diphenyl phosphite onto an alkyl bromide. *b*) DBU, MeCN, 0 °C to 20 °C, overnight, 26%. Panel C shows the normalized activity of DEBS TE for hydrolysis of **4** following an 18 h pre-treatment with diphenyl phosphonates.

Amino phosphonate **10** proved challenging to access. While phosphonates **3**, **5-7** were easily accessed via addition of commercially available Grignard and alkyl-lithium to

diphenyl phosphoryl chloride, accessing **10** via nucleophilic addition to diphenyl phosphoryl chloride was unsuccessful. We thus focused on an alkylation route involving addition of the cesium salt of diphenylphosphite to alkyl halides, as described by Salvatore *et al.* [26] While this proved successful and provided sufficient quantities of **10** for completion of the study, the reaction suffered from competing O-alkylation.

As the phosphonates are expected to modify the active site Ser₁₄₂, treatment of DEBS TE with the phosphonates should inhibit enzymatic activity. DEBS TE was treated with phosphonates or a vehicle control for 18 h and subsequently evaluated as to its ability to hydrolyze the *N*-acetyl cysteamine thioester of 3-hydroxyheptanoate, **4**. The normalized initial velocities relative to the DMSO control (Figure 4C) show that 18-hour treatment with most phosphonates inhibit DEBS TE activity. The diphenyl allylphosphonate **3** was particularly noteworthy, and inhibited DEBS TE by approximately 87 %.

Structure in complex with an diphenyl allylphosphonate

Treatment of TE₁₅₋₂₈₂ with diphenyl allylphosphonate **3**, similarly led to a loss of activity ($(V/[E]_t) = 0.03 \text{ min}^{-1}$, 88 % inhibition) demonstrating that DEBS₁₅₋₂₈₂ TE is also inhibited by diphenyl phosphonates (Figure 2). Based on this result, soaking experiments with **3** and TE₁₅₋₂₈₂ were performed and the resulting structure determined at a resolution of 2.1 Å (Table 1) (PDB ID: 5D3Z). The electron density map unambiguously indicates that the active site Ser of the TE was modified by **3** (Figure 5). The density indicates that both phenyl groups are absent, and the allyl chain becomes disordered after the first carbon. One of the phosphonate oxygens is within hydrogen bonding distance of His₂₅₉ of

the catalytic triad, and the other is making water-mediated hydrogen bonds to the hydroxyl side chain of Thr₇₆ and the backbone amides of Thr₇₆ and Ala₇₇. Otherwise, there are no other contacts between the allylphosphonate and the enzyme, and no structural differences between the unliganded and allylphosphonate-bound TE₁₅₋₂₈₂. The lack of structural rearrangement upon ligand binding is consistent with similar observations with Pik-TE and the phosphonate biosynthetic pathway,[22,23] but is seemingly at odds with the induced-fit mechanism for substrate recognition originally proposed for these enzymes.[20]

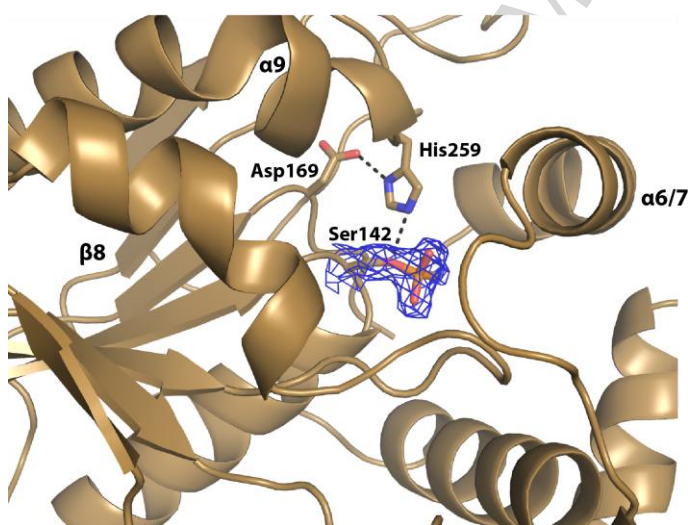


Figure 5. Electron density shows the allylphosphonate covalently bound to catalytic Ser₁₄₂ at the active site of TE₁₅₋₂₈₃.

Synthesis of complex phosphonates

The success of generating high-resolution structural data from soaking of TE₁₅₋₂₈₃ crystals with **3** encouraged us to synthesize more complex phosphonate analogues. Pinto *et al.* previously identified a set of diastereomeric substrates where the *syn* diastereomer

(Figure S3, **S1**) was macrocyclized by DEBS TE and the *anti* diastereomer (Figure S3, **S3**) was hydrolysed and not macrocyclized by DEBS TE (Figure S3, **S4**).[17] We thus expected that the diphenyl phosphonate analogs of these substrates, **1** and **2**, would provide us with the ideal set of compounds to identify the molecular basis for intramolecular cyclization.

Phosphonates **1** and **2** were synthesized using a convergent strategy that relied on coupling of diphenyl 6-aminohexylphosphonate (**16**) to both the *syn* and *anti* diastereomers of a protected 3,5-dihydroxy carboxylic acid (Figure 6). The two carboxylic acids were synthesized following similar routes, both involving sequential asymmetric Brown allylations to set the required stereogenic centers. Both syntheses began with an *in-situ* asymmetric Brown allylation of phenylacetaldehyde, **11**. [27] The homoallylic alcohol was then protected as a silyl ether (**12**) and the olefin was oxidatively cleaved to give aldehyde **13**. [28] A second Brown allylation followed by silylation was used to install the *syn* configured 1,3-diol functionality in **14**. While **14** was produced with *in-situ* preparation of the (-)ipc₂allyl borane, the *anti* substrate (**anti-14**) was produced using the commercially obtained (+)ipc₂allyl borane followed by silylation. [29] In our hands the *in-situ* preparation of (+)ipc₂allyl borane led to lower stereoselectivity with this substrate. The protected diols **14** and **anti-14** were subjected to oxidative cleavage of the olefin followed by Pinnick oxidation [30] to give the two acids **15** and **anti-15**.

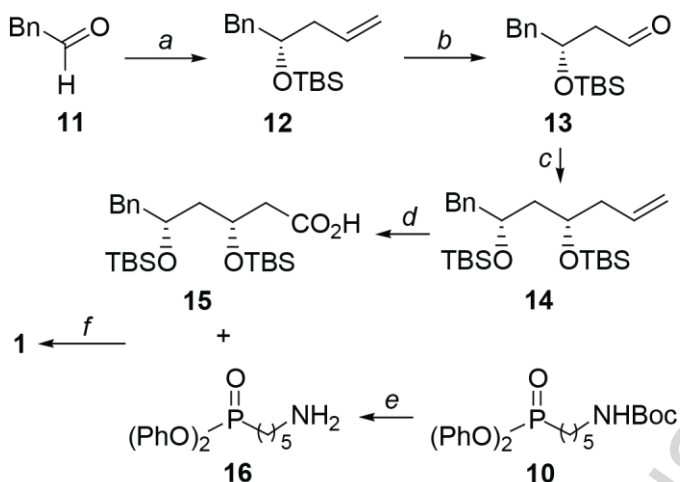


Figure 6. The synthesis of phosphonate **1** is shown. Phosphonate **2** was synthesized from **13** using following similar chemistry. *a*) 1. (-)-(Ipc)₂BOMe, allylMgBr, Et₂O, 0 °C, 1h; then phenylacetaldehyde, Et₂O, -100 °C, 2h; 2. Imidazole, TBSCl, DMF, r.t., overnight, 55% *b*) K₂CO₃, K₃Fe(CN)₆, K₂OsO₇•(H₂O)₂, 1:1 *t*-BuOH:H₂O, rt, overnight; then Pb(OAc)₄, DCM, 0.5h 54% *c*) 1.(-)-(Ipc)₂BOMe, allylMgBr, Et₂O, 0 °C, 1h; then phenylacetaldehyde, Et₂O, -100 °C, 2h; 2. Imidazole, TBSCl, DMF, r.t., overnight, 40% *d*) 1. K₂CO₃, K₃Fe(CN)₆, K₂OsO₇•(H₂O)₂, 1:1 *t*-BuOH:H₂O, rt, 12h; then Pb(OAc)₄, DCM, 0.5h; 2. NaClO₂, NaH₂PO₄, H₂O, 2-methyl-2-butene, *t*-BuOH, r.t., overnight, 63% *e*) HCl•Dioxane, r.t., 1h, *f*) 1. TBTU, DIEA, DMF, r.t., overnight 2. HF, pyridine, MeCN, r.t., 5h, 28% over 2 steps.

Completion of the synthesis required coupling the carboxylic acids (**15**, *anti*-**15**) with deprotected amino phosphonate. Deprotection of **7** was effected with HCl-dioxane and the free amine, **16**, was coupled to both **15** and *anti*-**15** using standard peptide coupling conditions (TBTU, DIEA), producing the fully protected *syn* and *anti*-phosphonates. Removal of the silyl ethers via treatment with HF and pyridine in acetonitrile[17] produced the final substrates **1** and **2**.

1 and **2** both inhibited TE activity. Pretreatment of TE₁₅₋₂₈₃ with **1** and **2** for 18 hours abolished enzymatic activity for hydrolysis of the *N*-acetyl cysteamine thioester of 3-hydroxyheptanoate **4** (Figure 2). This data suggests that the substrates can access the active site and modify the active site Ser as expected.

Soaking, co-crystallization, and mass spectrometry experiments with **1** and **2**

Based on these encouraging results, the structural characterization of the DEBS TE₁₅₋₂₈₃ in complex with **1** and **2** was initiated. Crystals were soaked in crystallization solutions supplemented with 5 mM of **1** and **2** individually. Soaking times between 1 and 14 days were investigated, and X-ray diffraction datasets were collected and processed. Analysis of the electron density maps did not show any additional densities in the active site.

We next attempted to form the acyl-enzyme intermediate in solution prior to crystallization. TE₁₅₋₂₈₃ was incubated with 5 mM **1** and **2** individually, which completely inhibited TE₁₅₋₂₈₃ activity. The ligand-enzyme complex was purified by gel filtration, crystallized using the same conditions as for the unmodified protein, and the structure was determined. Once again, no additional electron density was observed in the active site, despite the fact that the complex between the protein and the phosphonate was initially formed in solution.

To evaluate the stability of the complex, TE₁₅₋₂₈₃ was incubated with **1** to achieve full inhibition. The complex was then exchanged into a buffer containing all the components present during crystallization, with a reduced concentration of PEG to allow TE₁₅₋₂₈₃ to remain soluble, and the complex was kept at room temperature for 14 days, which is the approximate length of time required for crystal growth. Activity assays were then performed with TE₁₅₋₂₈₃ that had and had not been modified with **1**, before and after the 14 day incubation in crystallization-like conditions. Surprisingly, TE₁₅₋₂₈₃ regained

complete activity after the 14 day incubation in crystallization-like conditions, indicating that the alkylphosphonate had been lost from the active site Ser (Figure 7). Replacing individual components of the crystallization-like matrix (buffer: MES pH=6.5, HCl/Tris pH=8 – Precipitants: CaCl₂, Na-acetate, K-acetate, PEG-400, PEG-500 MME) did not suppress phosphonate hydrolysis.

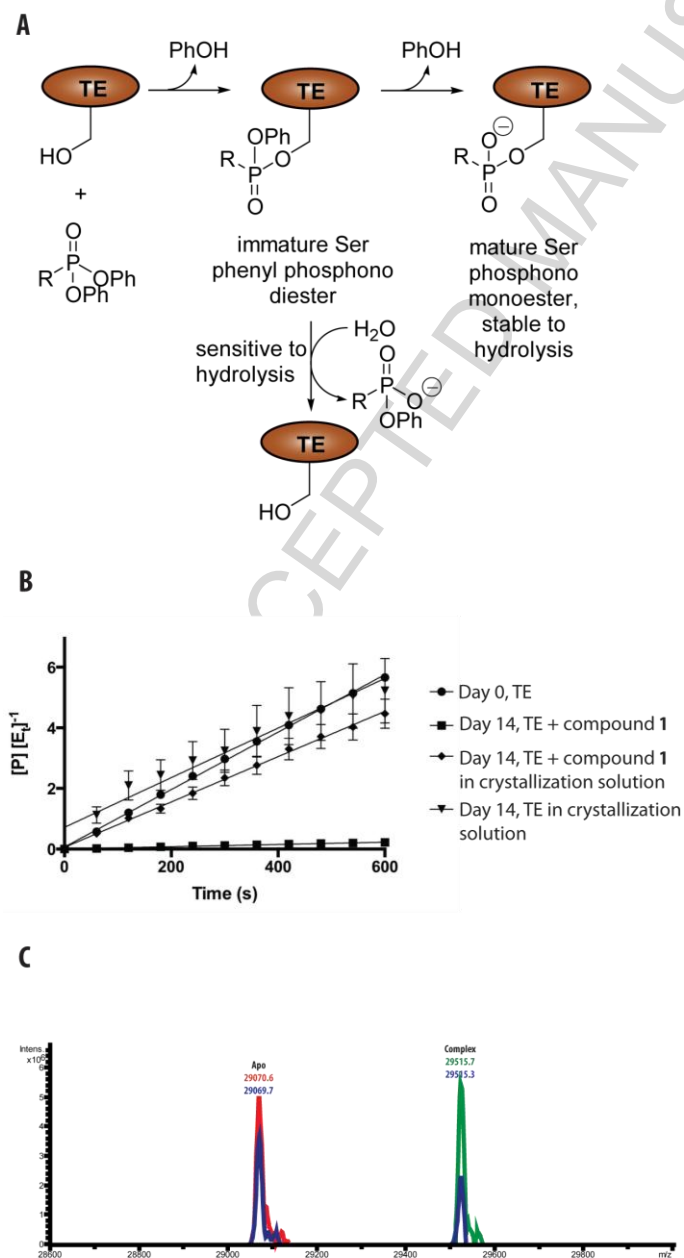


Figure 7. DEBS TE loses the phenyl alkylphosphono diester modification over time. Panel A shows how diphenyl phosphonate inhibitors can proceed through immature phenyl phosphono diester attached to Ser₁₄₂, to give either to mature, stable phosphono monoester attached to Ser₁₄₂ (though loss of a phenyl) or to an unmodified protein (through hydrolysis of the phenyl phosphono diester). Panel B shows the hydrolysis activity of TE₁₅₋₂₈₃ without inhibitor (circles; active for hydrolysis), of TE₁₅₋₂₈₃ treated with inhibitor, washed, and incubated in acylation buffer for 14 days (squares, largely inhibited), and of TE₁₅₋₂₈₃ treated with inhibitor in crystallization-like buffer for 14 days (diamonds, inhibition relieved). A control of TE₁₅₋₂₈₃ that was not modified and was incubated crystallization-like buffer for 14 days (triangle, active in hydrolysis) is also shown. Panel C shows mass spectra of intact TE₁₅₋₂₈₃ that was not treated with **1** (red), TE₁₅₋₂₈₃ that was treated with **1** (green), and TE₁₅₋₂₈₃ that was treated with **1** and incubated for 7 days in crystallization-like solution (blue). The MS data indicate progression from unmodified protein (apo-TE₁₅₋₂₈₃) to phenyl phosphono diester-TE TE₁₅₋₂₈₃, back to unmodified protein. Traces have been scaled to equal the same area under the curve as for the untreated (red) protein.

The putative mechanism for phosphonate formation on active site Ser occurs via two steps (Figure 7). The first step involves reversible phosphorylation of the Ser by the diphenyl phosphonate ester, such as **1**, **2**, and **3**, releasing a single equivalent of phenol.[31] In the second step, a second equivalent of phenol is released, generating the mature Ser phosphonomonoester, which is thought to be non-labile.[32,33] Based on this mechanism paradigm, and the observation of the monophenyl phosphonate ester, we propose that following has occurred in our experiments: The immature Ser phenyl phosphonodiester is formed when TE₁₅₋₂₈₃ is treated with **1** or **2**. This immature intermediate is then very slow to mature to the non-hydrolyzable Ser phosphonomonoester and under crystallization conditions, the faster, competing hydrolysis reaction leads to the removal of the immature diester to generate free TE₁₅₋₂₈₃ and the monophenyl phosphonate esters of **1** and **2**.

To test whether this competition is a likely reason for the lack of observed electron density in crystallography experiments with **1** and **2**, we performed whole protein mass spectrometric analyses of unmodified and modified TE₁₅₋₂₈₃ (Figure 7C, S4). Upon incubation with **1**, there is an increase in observed m/z for the protein of ~446 Da, the mass of the monophenyl phosphonate ester of **1** (C₂₄H₃₃NO₅P). After 7 days in crystallization-like buffer, most of TE₁₅₋₂₈₃ losses the monophenyl phosphonate ester and returns to the unmodified TE₁₅₋₂₈₃ m/z . No peak corresponding to the m/z of the mature non-hydrolysable phosphonomonoester is observed at the expected m/z of 29440 (increase of 370 Da to the unmodified TE₁₅₋₂₈₃ mass). This indicates that hydrolysis of the immature diester is favoured over maturation to the phosphonomonoester of **1** and **2**. In contrast, the diphenyl allylphosphonate derived immature TE₁₅₋₂₈₃ complex appears to undergo maturation to the non-hydrolyzable phosphonomonoester more rapidly and can be clearly seen electron density maps (Figure 5). Use of the more reactive phosphofluoridates may circumvent this limitation of diphenyl phosphonates by more rapidly accessing the non-hydrolyzable seryl-phosphonate monoester in both simple and complex inhibitors.[34–36]

Conclusion:

Obtaining high-resolution structural information on the enzyme-substrate interactions that govern the TE-mediated release of products in polyketide biosynthesis is essential to understand how these powerful catalysts function. We used phosphonate-based non-hydrolyzable acyl-enzyme intermediates in an attempt to gain insight into this product release. Our strategy led to a new construct of the DEBS TE with uncomplexed structure

determined at much higher resolution than those previously published and a high resolution structure of a simple allyl-enzyme intermediate. Using multistep stereoselective organic synthesis, we were able to obtain the complex phosphonate esters **1** and **2** that were close structural homologs of substrates known to undergo macrocyclization and hydrolysis. These phosphonate esters effectively inhibited the enzyme, but did not lead to co-complex structures. We suggest that the maturation of the labile phenyl seryl-phosphonate diester intermediate into the non-hydrolyzable seryl-phosphonate monoester product was slower than hydrolysis of the phenyl seryl-phosphonate diester, thus liberating free enzyme during crystallization. This result indicates that for successful application of phosphonate esters in characterizing acyl-enzyme intermediates, there is a delicate balance between maturation of the initial intermediate and its hydrolysis.

Methods

Synthesis of novel inhibitors the TE domain of DEBS

Reactions were carried out under argon or nitrogen atmosphere with dry solvents and dried glassware under anhydrous conditions unless specified otherwise. Reaction solvents THF, Et₂O and DCM were dried through activated alumina columns. Reagents were purchased at the highest commercial quality and used without further purification. Reactions were monitored by thin-layer chromatography (TLC) carried out on 0.25 mm E. Merck silica gel plates (60F-254) using UV light for visualization and/or ceric ammonium molybdate (CAM), *p*-anisaldehyde (PA) and potassium permanganate (KMnO₄) as staining solutions. Flash chromatography was performed with E. Merck silica

gel (60, particle size 0.040-0.063 mm) and preparative thin-layer chromatography (PTLC) separations were carried out on 0.25 mm E. Merck silica gel plates (60F-254).

^1H NMR, ^{13}C NMR, ^{31}P NMR spectra were recorded on the Bruker DPX-300, AMX-300, AMX-300II, and AMX-400 spectrometers and calibrated using residual undeuterated solvents as internal references. Data is reported as follows: chemical shifts in ppm (δ); multiplicities are indicated by the following abbreviations: s = singlet, d = doublet, t = triplet, q = quartet, p = pentet, dd = doublet of doublets, dt = doublet of triplets, m = multiplet, br = broad; coupling constants (J) in Hz. Infrared spectra (IR) were collected on a Shimadzu FTIR-8400S in solution and reported in wavenumbers (cm^{-1}). HRMS were obtained on a Kratos Analytical Concept instrument (University of Ottawa Mass Spectrum Center).

HPLC data for enantiopurity were collected with an Agilent 1100 series HPLC with a DAD detector and Chiralpak IB column. The conditions for the separation were 98:2 Hexane:isopropyl alcohol at a rate of 0.8 mL/min and detection at 220 nm. MALDI-TOF traces were collected with a Bruker microflex LT with sinnapic acid sandwich. Spectrophotometric measurements were collected on a Thermo Scientific Evolution 300 UV-Vis spectrophotometer.

General procedure for formation of alkylphosphonates (3, 5-7)

To diphenyl phosphoryl chloride (1 equiv.) dissolved in ether (0.2 M) was added an alkyl Grignard (2.5 equiv.) at $-78\text{ }^\circ\text{C}$. The reaction was stirred for 3 hours and allowed to warm to room temperature. The reaction mixture was quenched with saturated

ammonium chloride (15 mL) and diluted with water. The aqueous layer was then extracted with EtOAc (3×10 mL) and the resulting organic layer washed with brine (2×10 mL), dried with MgSO_4 and concentrated *in vacuo*. The product was purified by flash column chromatography.

Diphenyl allylphosphonate (3):

The procedure outlined above was employed for the reaction between diphenyl phosphoryl chloride (0.5 mL, 2.41 mmol, 1 equiv.) and allylmagnesium bromide (6.0 mL, 6.03 mmol, 2.5 equiv) yielding 0.106 g (0.38 mmol, 16%) of diphenyl allylphosphonate **3**. $R_f = 0.24$ (silica gel, 20% EtOAc/Hex); ^1H NMR (400 MHz, CDCl_3): δ 7.32-7.28 (m, 4H), 7.16-7.12 (m, 6H), 6.02-5.94 (m, 1H), 5.34-5.42-5.33 (m, 2H), 3.01 (dt, $J = 7.4, 1.4$ Hz) ppm; ^{13}C NMR (100 MHz, CDCl_3): δ 129.8, 126.3, 125.2, 125.2, 121.4, 120.6, 32.4, 31.0 ppm. NMR spectra are consistent with those previously reported.[37]

Diphenyl hexylphosphonate (5)

The procedure outlined above was employed for the reaction between diphenyl phosphoryl chloride (0.5 mL, 2.41 mmol, 1 equiv.) with hexylmagnesium bromide (3.0 mL, 6.03 mmol, 2.5 equiv) yielding 0.143 g (0.46 mmol, 19%) of diphenyl hexylphosphonate **5**. $R_f: 0.35$ (silica gel, 15% (EtOAc/Hex); ^1H NMR (400 MHz, CDCl_3): δ 7.33-7.27 (m, 4H), 7.16-7.12 (m, 6H), 2.11-1.98 (m, 2H), 1.83-1.72 (m, 2H), 1.50-1.18 (m, 9H) ppm; ^{13}C NMR (100 MHz, CDCl_3): δ 150.2, 130.0, 124.8, 121.1, 36.0,

29.2, 26.8, 26.0, 25.8, 25.7, 25.6 ppm. NMR spectra are consistent with those previously reported.[38]

Diphenyl cyclohexylphosphonate (6)

The procedure outlined above was employed for the reaction between diphenyl phosphoryl chloride (0.5 mL, 2.41 mmol, 1 equiv.) with cyclohexylmagnesium bromide (3.0 mL, 6.03 mmol, 2.5 equiv) yielding 0.136 g (0.42 mmol, 15%) of diphenyl cyclohexylphosphonate **6**. R_f : 0.36, (silica gel, 15% (EtOAc/Hex)); ^1H NMR (400 MHz, CDCl_3): δ 7.31-7.26 (m, 4H), 7.16-7.12 (m, 6H), 2.21-2.09 (m, 1H), 1.92-1.84 (m, 4H), 1.50-1.32 (m, 6H) ppm. ^{13}C NMR (100 MHz, CDCl_3): δ 150.4, 129.6, 124.7, 120.6, 36.0, 29.2, 25.8, 25.7, 25.6 ppm. NMR spectra are consistent with those previously reported.[39]

Diphenyl phenylphosphonate (7)

The procedure outlined above δ (0.5 mL, 2.41 mmol, 1 equiv.) with phenyl lithium (2.4 mL, 6.03 mmol, 2.5 equiv) yielding 0.105 g (0.34 mmol, 14%) of diphenyl phenylphosphonate **7**. R_f : 0.25, (silica gel, 20% (EtOAc/Hex)); ^1H NMR (400 MHz, CDCl_3): δ 7.32-7.27 (m, 4H), 7.16-7.12 (m, 6H) ppm; ^{13}C NMR (100 MHz, CDCl_3): δ 150.4, 150.4, 133.2, 132.3, 132.2, 129.7, 128.7, 128.6, 125.1, 120.7, 120.6 ppm. NMR spectra are consistent with those previously reported.[40]

1-bromo-6-(tert-butoxycarbonylamino)-hexane (9)

To 6-aminohexan-1-ol (0.500 g, 2.82 mmol, 1 equiv.) dissolved in a 1:1 dioxane/water mixture (12 mL) was added K_2CO_3 (1.870 g, 13.56 mmol, 4 equiv.) and mixed at room temperature for 10 minutes. Di-tert-butyl dicarbonate (0.7 mL, 3.39 mmol, 1.2 equiv.) was added to the mixture and allowed to mix overnight. The reaction was diluted with EtOAc (12 mL) and the organic layer separated. The layer was washed with 10 % HCl (2×10 mL), dried over $MgSO_4$ and concentrated in vacuo. The reaction yield was 0.570 g (2.62 mmol, 93%) and the product was taken onto the next step without further purification. R_f : 0.50, (silica gel, 60% (EtOAc/Hex)); 1H NMR (400 MHz, $CDCl_3$): δ 4.51 (br s, 1H), 3.61 (t, $J = 6.5$ Hz, 2H), 3.09 (t, $J = 6.7$ Hz, 2H), 1.42 (s, 9H), 1.55-1.30 (m, 8H) ppm; ^{13}C NMR (100 MHz, $CDCl_3$): δ 156.1, 79.0, 62.7, 40.4, 32.6, 30.1, 28.4, 26.4, 25.3 ppm. NMR spectra are consistent with those previously reported.[41]

To 6-(tert-butoxycarbonylamino)hexan-1-ol (0.600 g, 2.76 mmol, 1 equiv.) in dry dichloromethane (14 mL) was added CBr_4 (0.920 g, 2.76 mmol, 1 equiv.) and PPh_3 (0.720 g, 2.76 mmol, 1 equiv.) at 0 °C. The resulting mixture was allowed to warm to room temperature over 2 hours. The reaction was concentrated in vacuo and purified by column chromatography to yield 0.696 g of **9** (2.48 mmol, 90%). R_f : 0.57, (silica gel, 20% (EtOAc/Hex)); 1H NMR (400 MHz, $CDCl_3$): δ 4.48 (br s), 3.66 (t, $J = 6.8$ Hz, 2H), 3.09 (t, $J = 6.5$ Hz, 2H), 1.88-1.82 (m, 2H), 1.47 (s, 9H), 1.54-1.18 (m, 6H) ppm; ^{13}C NMR (100 MHz, $CDCl_3$): δ 156.1, 62.9, 51.1, 32.8, 28.5, 26.4, 25.4 ppm. NMR spectra are consistent with those previously reported.[42]

6-(tert-butoxycarbonylamino)-1-diphenoxyphoryl hexane (10)

To diphenylphosphite (0.2 mL, 1.04 mmol, 1 equiv.) in acetonitrile (4 mL) was added DBU (0.18 mL, 1.15 mmol, 1.1 equiv.) at 0 °C. This solution was mixed for 10 minutes and 1-bromo-6-(di-tert-butoxycarbonylamino)hexane (0.18 mL, 1.15 mmol, 1.1 equiv.) was added slowly over 10 minutes. The resulting mixture was allowed to warm to room temperature and stirred overnight. The reaction was diluted with H₂O (3 mL), extracted with EtOAc (3 × 5 mL) and washed with 10% HCl (2 × 5 mL) and brine (2 × 5 mL). The resulting organic layer was dried over MgSO₄, concentrated in vacuo and purified by column chromatography to yield 0.126 g of **10** (0.29 mmol, 28%). R_f: 0.50, (silica gel, 60% (EtOAc/Hex)); ¹H NMR (400 MHz, CDCl₃): δ 7.32-7.28 (m, 4H), 7.16-7.13 (m, 6H), 4.48 (s, 1H, -NH), 3.09 (t, *J* = 6.0 Hz, 2H), 2.11-2.00 (m, 2H), 1.83-1.73 (m, 2H), 1.57-1.42 (m, 3H), 1.36 (s, 9H), 1.35-1.33 (m, 3H) ppm; ¹³C NMR (100 MHz, CDCl₃): δ 156.0, 150.4, 129.8, 125.1, 120.6, 120.5, 77.23, 30.2, 30.0, 26.5, 26.2, 25.2, 22.3, 22.3 ppm; ³¹P NMR (121 MHz, CDCl₃): δ 25.80 (tt, *J* = 17.4, 12.5 Hz) ppm. HRMS (EI) *m/z* calcd for C₂₃H₃₂NO₅P [M+H]⁺ 434.2096, found 434.1998.

(R)-2-(tert-Butyldimethylsilyloxy)-1-phenylpent-4-ene (12):

To (-)-B-methoxydisopinocampheylborane (5.0 g, 15.81 mmol, 1.25 equiv.) dissolved in ether (15.2 mL) was added allylmagnesium bromide (15.2 mL, 15.2 mmol, 1.20 equiv.) and stirred vigorously at 0 °C for 1 hour. A large amount of white solid (presumably MgBrOMe) precipitates upon addition of the allylmagnesium bromide. The

reaction was allowed to warm to room temperature over 2 hours. A solution of phenylacetaldehyde (1.5 mL, 12.65 mmol, 1 equiv.) in ether (9.7 mL) and the reaction are cooled to -100°C. The phenylacetaldehyde solution was added dropwise to the borane solution ensuring that the temperature remains at -100 °C. The ether/liquid N₂ bath was maintained for 1 hour and then allowed to warm to room temperature. A solution of 15 % NaOH (6 mL) and 30 % H₂O₂ (9 mL) was premixed and added to the reaction dropwise at 0 °C to ensure the vigorous reaction does not overflow. This mixture was equipped with a water condenser and refluxed for 45 minutes. The reaction was diluted with EtOAc (12 mL) and the aqueous layer extracted with EtOAc (2 × 20 mL). The organic layer was washed with NaCl (2 × 15 mL), dried over MgSO₄ and concentrated in vacuo. The product was purified by flash column chromatography (2% EtOAc/Hexanes) to yield 1.26 g of (*R*)-1-phenylpent-4-en-2-ol (7.5 mmol, 60%) Chiral HPLC analysis showed the compound to have 85% *ee* (See SI for data). R_f: 0.38, (silica gel, 10% (EtOAc/Hex)); ¹H NMR (400 MHz, CDCl₃): δ 7.33-7.19 (m, 5H), 5.92-5.79 (m, 1H), 5.18-5.14 (m, 1H), 5.12 (t, *J* = 1.2 Hz, 1H), 3.92-3.83 (m, 1H), 2.84-2.68 (m, 2H), 2.37-2.29 (m, 1H), 2.25-2.16 (m, 1H), 1.62 (br s, 1H) ppm; ¹³C NMR (100 MHz, CDCl₃): δ 138.4, 134.7, 129.4, 128.6, 126.5, 118.2, 71.7, 43.3, 41.2 ppm. NMR spectra are consistent with those previously reported.[17]

To (*R*)-1-phenylpent-4-en-2-ol (2.13g, 13.13 mmol, 1 equiv.) dissolved in anhydrous DMF (13.1 mL) was added imidazole (1.97 g, 28.89 mmol, 2.2 equiv.) and TBSCl (2.97 g, 19.70 mmol, 1.5 equiv.) at room temperature and mixed overnight. After checking by TLC for completion, the reaction mixture was quenched with saturated

ammonium chloride (15 mL) and diluted with EtOAc. The aqueous layer was then extracted with EtOAc and the resulting organic layer washed with water whilst increasing the concentration of brine to 100%. The organic layer was dried with MgSO₄ and concentrated in vacuo. The product was purified by flash column chromatography (2% EtOAc/Hexanes) to yield 3.34 g of **12** (12.08 mmol, 92%). **R_f**: 0.22, (silica gel, 10% (EtOAc/Hex)); ¹H NMR (400 MHz, CDCl₃): δ 7.27-7.14 (m, 5H), 5.88-5.80 (m, 1H), 5.07-5.01 (m, 2H), 3.88-3.84 (m, 1H), 2.78-2.63 (m, 2H), 2.34-2.18 (m, 2H), 0.82 (s, 9H) -0.08 (s, 3H) -0.25 (s, 3H) ppm; ¹³C NMR (100 MHz, CDCl₃): δ 139.3, 135.1, 129.9, 128.1, 126.1, 117.1, 73.5, 43.6, 41.7, 41.7, 26.0, 18.1, -4.8, -5.1 ppm. HRMS (EI) *m/z* calcd for C₁₆H₂₆O₂Si [M+H]⁺ 219.1200, found 219.1192.

(S)-3-tert-Butyldimethylsilyl-5-phenylpentan-1-al (**13**)

To **12** (1.26 g, 4.56 mmol, 1 equiv.) dissolved in anhydrous 1:1 ^tBuOH:H₂O (46 mL) was added K₂CO₃ (1.89 g, 13.68 mmol, 3 equiv.) and K₃Fe(CN)₆ (4.50 g, 13.68 mmol, 3 equiv.) at room temperature. The reaction was stirred at room temperature until most of the solid was dissolved followed by the addition of K₂OsO₇•(H₂O)₂ (0.020 g, 0.05 mmol, 0.01 equiv.) in 15% NaOH (1.5 mL), which was mixed overnight. After checking by TLC for completion, the reaction mixture was diluted with H₂O and extracted with EtOAc (3 × 30 mL). The pooled organic layer was washed with brine, dried with MgSO₄ and concentrated in vacuo. The product was then dissolved in DCM (18 mL) and Pd(OAc)₄ (2.43 g, 5.47 mmol, 1.2 equiv.) and stirred for 1 hour. The reaction was then concentrated in vacuo, redissolved in EtOAc, silica gel was added, and the solvent evaporated in vacuo. The dry silica was loaded onto a flash column and the

product purified by flash column chromatography (5% EtOAc/Hexanes) to yield 0.686 g of **13** (2.46 mmol, 54%). R_f : 0.45, (silica gel, 10% (EtOAc/Hex)); ^1H NMR (400 MHz, CDCl_3): δ 9.76 (t, $J = 2.6$ Hz, 1H), 7.29-7.13 (m, 5H), 4.36 (p, $J = 6.2$ Hz, 1H), 2.88-2.74 (m, 2H), 2.49 (dd, $J = 5.7, 2.5$ Hz, 2H), 0.84 (s, 9H) -0.01 (s, 3H) -0.12 (s, 3H) ppm. ^{13}C NMR (100 MHz, CDCl_3): δ 202.0, 137.8, 129.7, 128.4, 69.6, 50.6, 44.6, 25.8, 18.0, -4.8, -4.9 ppm; HRMS (EI) m/z calcd for $\text{C}_{16}\text{H}_{26}\text{O}_2\text{Si}$ $[\text{M}+\text{H}]^+$ 277.1701, found 277.1610.

(4*S*,6*S*)-4,6-Bis(tert-butyltrimethylsilyloxy)-7-phenylhept-1-ene (**14**)

To (-)-B-methoxydisopinocampheylborane (2.33 g, 7.36 mmol, 1.25 equiv.) dissolved in ether (7.4 mL) was added allylmagnesium bromide (7.0 mL, 7.0 mmol, 1.20 equiv.) and the reaction was stirred vigorously at 0 °C for 1 hour. A large amount of white solid (presumably MgBrOMe) precipitated upon addition of the allylmagnesium bromide. The reaction was allowed to warm to room temperature over 2 hours. A solution of **13** (1.64 g, 5.89 mmol, 1 equiv.) in ether (4.5 mL) and the borane reaction were both cooled to -100 °C. The aldehyde solution was added dropwise to the borane reaction ensuring that the temperature remained at -100 °C. An ether/liquid N_2 bath was maintained for 1 hour and then the reaction was allowed to warm to room temperature. A solution of 15% NaOH (6 mL) and 30% H_2O_2 (9 mL) was premixed and added to the reaction dropwise at 0 °C to ensure the vigorous reaction does not overflow. This mixture was equipped with a water condenser and refluxed for 45 minutes. The reaction was diluted with EtOAc (12 mL) and the aqueous layer extracted with EtOAc (2×20 mL) The organic layer was washed with NaCl (2×15 mL), dried over MgSO_4 and concentrated in vacuo. The product was purified by flash column chromatography (2% EtOAc/Hexanes) to yield

1.170 g of (4*S*,6*S*)-6-(tert-butyldimethylsilyloxy)-7-phenylhept-1-en-4-ol (3.65 mmol, 62%). R_f : 0.38, (silica gel, 10% (EtOAc/Hex)); ^1H NMR (400 MHz, CDCl_3): δ 7.46-7.07 (m, 5H), 5.89-5.66 (m, 1H), 5.17-4.96 (m, 2H), 4.15-4.02 (m, 1H), 3.82-3.71 (m, 1H), 2.91-2.65 (m, 2H), 2.19-2.08 (m, 2H), 1.64-2.06 (m, 2H) 0.88 (s,9H) 0.08 (s,3H) -0.00 (s,3H) ppm; ^{13}C NMR (100 MHz, CDCl_3): δ 138.6, 134.9, 129.7, 128.8, 126.5, 117.8, 74.0, 70.1, 44.9, 43.2, 42.8, 41.9, 26.0, -3.9, -4.7 ppm. NMR spectra are consistent with those previously reported.[17]

To (4*S*,6*S*)-6-(tert-butyldimethylsilyloxy)-7-phenylhept-1-en-4-ol (1.09 g, 3.56 mmol, 1 equiv.) dissolved in anhydrous DMF (3.6 mL) was added imidazole (0.53 g, 7.82 mmol, 2.2 equiv.) and TBSCl (0.65 g, 4.27 mmol, 1.2 equiv.) at room temperature and mixed overnight. After checking by TLC for completion, the reaction mixture was quenched with saturated ammonium chloride (15 mL) and diluted with EtOAc. The aqueous layer was then extracted with EtOAc and the resulting organic layer washed with water whilst increasing the concentration of brine to 100%. The organic layer was then dried with MgSO_4 and concentrated in vacuo. The product was purified by flash column chromatography (2% EtOAc/Hexanes) to yield 1.01 g of **14** (2.31 mmol, 65%). R_f : 0.63, (silica gel, 5% (EtOAc/Hex)); ^1H NMR (400 MHz, CDCl_3): δ 7.26-7.13 (m, 5H), 5.73-5.70 (m, 1H), 4.99-4.93 (m, 2H), 3.94-3.91 (m, 1H), 3.86-3.83 (m, 1H), 2.78-2.63 (m, 2H), 2.22-2.20(m, 2H), 0.87 (s, 9H), 0.82 (s, 9H), 0.06 (s, 3H), 0.04 (s, 3H), -0.07 (s, 3H), -0.20 (s, 3H) ppm. ^{13}C NMR (100 MHz, CDCl_3): δ 139.1, 134.8, 129.9, 128.1, 126.0, 117.0, 70.9, 69.1, 44.5, 44.2, 42.0, 25.9, 18.1, -4.2, -4.4, -4.7, -4.8 ppm; HRMS (EI) m/z calcd for $\text{C}_{20}\text{H}_{35}\text{O}_4\text{Si}_2$ $[\text{M}+\text{H}]^+$ 377.2327, found 377.2310.

(4*S*,6*R*)-4,6-Bis(tert-butyldimethylsilyloxy)-7-phenylhept-1-ene (*anti*-14)

To (4*S*,6*R*)-6-(tert-butyldimethylsilyloxy)-7-phenylhept-1-en-4-ol (1.20 g, 4.31 mmol, 1 equiv.) dissolved in anhydrous ether (14 mL) was added (+)-Ipc₂BAllyl (5.0 mL, 5.00 mmol, 1.2 equiv.) at -100 °C. The ether/liquid N₂ bath was maintained for 1 hour and then allowed to warm to room temperature. A solution of 15% NaOH (3 mL) and 30% H₂O₂ (4.5 mL) was premixed and added to the reaction dropwise at 0 °C to ensure the vigorous reaction does not overflow. This mixture was equipped with a water condenser and refluxed for 45 minutes. The reaction was diluted with EtOAc (12 mL) and the aqueous layer extracted with EtOAc (2 × 20 mL). The organic layer was washed with NaCl (2 × 15 mL), dried over MgSO₄ and concentrated in vacuo. The product was purified by flash column chromatography (2% EtOAc/Hexanes) to yield 0.484 g of (4*S*,6*R*)-6-(tert-butyldimethylsilyloxy)-7-phenylhept-1-en-4-ol (1.51 mmol, 35%). R_f: 0.34, (silica gel, 10% (EtOAc/Hex); ¹H NMR (400 MHz, CDCl₃): δ 7.29-7.11 (m, 5H), 5.87-5.70 (m, 1H), 5.11-5.00 (m, 2H), 4.22-4.15 (m, 1H), 4.12-4.03 (m, 1H), 3.37-3.30 (d, *J* = 1.9 Hz, 1H) 2.95-2.75 (m, 2H), 2.26-2.07 (m, 2H), 1.57-1.52 (m, 2H) 0.86 (s, 9H) 0.03 (s, 3H) -0.15 (s, 3H) ppm; ¹³C NMR (100 MHz, CDCl₃): δ 138.8, 134.9, 129.7, 128.6, 126.5, 117.6, 73.1, 67.9, 43.2, 42.3, 40.8, 25.6, 18.2, -4.8 ppm. NMR Spectra are consistent with those previously reported.[17]

To (4*S*,6*R*)-6-(tert-butyldimethylsilyloxy)-7-phenylhept-1-en-4-ol (0.460 g, 3.56 mmol, 1 equiv.) dissolved in anhydrous DMF (1.5 mL) was added imidazole (0.22 g, 3.23 mmol, 2.2 equiv.) and TBSCl (0.26 g, 1.75 mmol, 1.2 equiv.) at room temperature and mixed overnight. After checking by TLC for completion, the reaction mixture was quenched with saturated ammonium chloride (15 mL) and diluted with EtOAc. The

aqueous layer was then extracted with EtOAc and the resulting organic layer washed with water whilst increasing the concentration of brine to 100%. The organic layer was dried with MgSO₄ and concentrated in vacuo. The product was purified by flash column chromatography (2% EtOAc/Hexanes) to yield 0.789 g of *anti-14* (1.82 mmol, 51%). R_f: 0.63, (silica gel, 5% (EtOAc/Hex)); ¹H NMR (400 MHz, CDCl₃): δ 7.27-7.12 (m, 5H), 5.82-5.72 (m, 1H), 5.05-4.97 (m, 2H), 3.95-3.91 (m, 1H), 3.85-3.77 (m, 1H), 2.73-2.71 (m, 2H), 2.23-2.19 (m, 2H), 1.63-1.54 (m, 2H), 0.82 (s, 9H), 0.82 (s, 9H), -0.01 (s, 3H), -0.02 (s, 3H), -0.04 (s, 3H), -0.17 (s, 3H) ppm; ¹³C NMR (100 MHz, CDCl₃): δ 139.1, 135.2, 130.0, 128.2, 126.1, 117.0, 71.6, 70.0, 45.0, 44.7, 42.5, 26.0, 18.1, -4.0, -4.3, -4.4 ppm. HRMS (EI) *m/z* calcd for C₂₀H₃₅O₄Si₂ [M+H]⁺ 377.2327, found 377.2560.

(4*S*,6*S*)-4,6-Bis(tert-butyldimethylsilyloxy)-7-phenylheptanoic acid (15)

To **14** (0.343 g, 0.66 mmol, 1 equiv.) dissolved in anhydrous 1:1 ^tBuOH:H₂O (8 mL) was added K₂CO₃ (0.332 g, 1.98 mmol, 3 equiv.) and K₃Fe(CN)₆ (0.782 g, 1.98 mmol, 3 equiv.) at room temperature. The reaction was stirred at room temperature until most of the solid was dissolved. This was followed by addition of K₂O₈O₇•(H₂O)₂ (0.006 g, 0.015 mmol, 0.02 equiv.) in 15% NaOH (1.5 mL) and the mixture was stirred overnight. After checking by TLC for completion, the reaction mixture was diluted with H₂O and extracted with EtOAc (3 × 30 mL). The pooled organic layers were washed with brine, dried with MgSO₄ and concentrated in vacuo. The product was then dissolved in DCM (3 mL), Pb(OAc)₄ (0.409 g, 0.91 mmol, 1.2 equiv.) was added, and the reaction stirred for 1 hour. The mixture was then concentrated in vacuo and the crude product was checked by NMR for the aldehyde peak.

This aldehyde (0.302 g, 0.65 mmol, 1 equiv.) was dissolved in ^tBuOH (9 mL). NaClO₂ (0.182 g, 1.99 mmol, 3 equiv.) and NaH₂PO₄ (0.483 g, 3.98 mmol, 6 equiv.) dissolved in water (2 mL) was then added drop wise over 5 minutes. 2-methyl-2-butene (3.3 mL, 6.61 mmol, 10 equiv.) was added to reaction and the mixture was allowed to stir at room temperature for 24 hours. The reaction was then washed with 10% HCl (2 × 2 mL) and diluted with DCM (4 mL). The aqueous layer is then extracted with DCM (3 × 4 mL) and the resulting organic layers were pooled and washed with brine (3 × 2 mL). The organic layer was dried with MgSO₄ and concentrated in vacuo. The product was purified by flash column chromatography (5% EtOAc/Hexanes) to yield 0.656 g of **15** (1.45 mmol, 63%). R_f: 0.12, (silica gel, 10% (EtOAc/Hex)); ¹H NMR (400 MHz, CDCl₃): δ 7.27-7.14 (m, 5H), 4.32-4.26 (m, 1H), 3.96-3.90 (m, 1H), 2.62-2.54 (m, 2H), 2.54-2.38 (m, 2H), 1.74-1.60 (m, 2H), 0.86 (s, 9H), 0.85 (s, 9H), 0.04 (s, 6H), -0.01 (s, 3H), -0.14 (s, 3H) ppm; ¹³C NMR (100 MHz, CDCl₃): δ 177.2, 138.5, 129.7, 128.3, 126.3, 70.6, 66.7, 44.4, 44.2, 42.3, 25.9, 25.8, -4.4, -4.7, -4.8 ppm. HRMS (EI) *m/z* calcd for C₂₀H₃₅O₄Si₂ [M+H]⁺ 395.2068, found 395.2050.

(4*S*,6*R*)-4,6-bis(tert-butyldimethylsilyloxy)-7-phenylheptanoic acid (*anti*-**15**)

To *anti*-**14** (0.33 g, 0.75 mmol, 1 equiv.) dissolved in anhydrous 1:1 ^tBuOH:H₂O (8 mL) was added K₂CO₃ (0.31 g, 2.26 mmol, 3 equiv.) and K₃Fe(CN)₆ (0.75 g, 2.26 mmol, 3 equiv.) at room temperature. The reaction was stirred at room temperature until most of the solid was dissolved. Following this K₂O₈O₇•(H₂O)₂ (0.005 g, 0.015 mmol, 0.02 equiv.) in 15% NaOH (1.5 mL) was added to the mixture and it was stirred overnight. After checking by TLC for completion, the reaction mixture was diluted with

H₂O and extracted with EtOAc (3 × 30 mL). The pooled organic layer was washed with brine dried with MgSO₄ and concentrated in vacuo. The product was then dissolved in DCM (3 mL) and Pb(OAc)₄ (0.40 g, 0.91 mmol, 1.2 equiv.) and stirred for 1 hour. The reaction was then concentrated in vacuo and the crude product was checked by NMR for the aldehyde peak.

The aldehyde (0.33 g, 0.72 mmol, 1 equiv.) was dissolved in ^tBuOH (9 mL). NaClO₂ (0.02 g, 2.17 mmol, 3 equiv.) and NaH₂PO₄ (0.05 g, 4.34 mmol, 6 equiv.) dissolved in water (2.2 mL) was added to the aldehyde drop wise over 5 minutes. 2-methyl-2-butene (3.6 mL, 7.24 mmol, 10 equiv.) was then added and the reaction was allowed to stir at room temperature for 24 hours. The mixture was then washed with 10% HCl (2 × 2 mL) and diluted with DCM (4 mL). The aqueous layer was then extracted with DCM (3 × 4 mL) and the resulting organic layers were pooled and washed with brine (3 × 2 mL). The organic layer is dried with MgSO₄ and concentrated in vacuo. The product was purified by flash column chromatography (5% EtOAc/Hexanes) to yield 0.149 g of *anti-15* (0.33 mmol, 44%). R_f: 0.12, (silica gel, 10% EtOAc/Hex); ¹H NMR (400 MHz, CDCl₃): δ 7.26-7.13 (m, 5H), 4.18-4.12 (m, 1H), 3.94-3.88 (m, 1H), 2.82-2.60 (m, 2H), 2.58-2.44 (m, 2H), 1.76-1.60 (m, 2H), 0.85 (s, 9H), 0.79 (s, 9H), 0.00 (s, 3H), -0.03 (s, 3H), -0.04 (s, 3H), -0.11 (s, 3H) ppm; ¹³C NMR (100 MHz, CDCl₃): δ 176.1, 138.5, 129.9, 128.3, 126.4, 71.7, 67.8, 44.9, 44.6, 42.9, 25.9, 25.7, -4.4, -4.5, -4.7 ppm; HRMS (EI) *m/z* calcd for C₂₀H₃₅O₄Si₂ [M+H]⁺ 395.2068, found 395.2061.

(3*S*,5*S*) Diphenyl (6-(3,5-dihydroxy-6-phenylhexanoylamino)hexylphosphonate (1)

Compound **10** (0.05 g, 0.13 mmol, 1.3 equiv) was dissolved in HCl/Dioxane (0.3 mL, 1.95 mmol, 13 equiv.) at room temperature under argon. After stirring for 1 hour, the solvent was evaporated in vacuo and the free amine **16** was used directly in the next reaction.

Compound **15** (0.04 g, 0.15 mmol, 1 equiv.) was dissolved in DMF (1.0 mL) and added drop wise to the freshly deprotected amine. TBTU (0.04 g, 0.18 mmol, 1.2 equiv.) and DIEA (50 μ L, 0.45 mmol, 3 equiv.) were added to this solution and the reaction was mixed under argon for 24 hours at room temperature. After checking by TLC for completion, the reaction mixture was poured over brine (10 mL) and extracted with EtOAc (3 \times 10 mL). The organic layer was dried with MgSO₄ and concentrated in vacuo. The product was purified by flash column chromatography (20% Acetone/Hexanes) to yield 0.043 g of (3*S*,5*S*) diphenyl (6-(3,5-bis(tert-butyldimethylsilyloxy)-6-phenylhexanoylamino)hexylphosphonate (0.056 mmol, 43%). R_f: 0.45, (silica gel, 30% Acetone/Hex); ¹H NMR (400 MHz, CDCl₃): δ 7.31-7.11 (m, 15H), 6.31 (br t, *J* = 5.1 Hz, 1H), 4.19-4.15 (m, 1H), 3.95-3.92 (m, 1H), 3.21-3.07 (m, 2H), 2.80-2.71 (m, 2H), 2.47-2.20 (m, 2H), 2.06-1.99 (m, 2H), 1.79-1.73 (m, 4H), 1.44-1.34 (m, 8H), 0.85 (s, 9H), 0.84 (s, 9H), 0.05 (s, 3H), 0.04 (s, 3H), -0.00 (s, 3H), -0.13 (s, 3H) ppm; ¹³C NMR (100 MHz, CDCl₃): δ 170.7, 150.4, 138.4, 129.8, 129.7, 128.2, 126.2, 125.1, 120.6, 120.5, 70.5, 67.2, 44.4, 43.6, 43.4, 39.1, 30.2, 30.0, 29.3, 26.6, 26.5, 25.9, 25.8, 22.3, 22.3, 18.0, 17.9, -4.6, -4.8 ppm. ³¹P NMR (121 MHz, CDCl₃): δ 25.70 (tt, *J* = 17.4, 12.5 Hz) ppm; HRMS (ESI) *m/z* calcd for C₃₆H₅₂NO₆PSi [M+H]⁺ 653.3302, found 653.9926.

(3*S*,5*S*) Diphenyl (6-(3,5-bis(tert-butyldimethylsilyloxy)-6-phenylhexanoylamino)hexylphosphonate (0.026 g, 0.034 mmol, 1 equiv.) was placed in

an Eppendorf tube and dissolved in MeCN (1.7 mL) at room temperature. Pyridine (55 μ L, 0.677 mmol, 10 equiv.) followed by 48 % aqueous HF (285 μ L, 6.77 mmol, 100 equiv.) were added to the reaction and the mixture was vortexed for 10 seconds. The reaction proceeded with no stirring for 5 hours. The reaction was then diluted with water (1 mL) extracted with EtOAc (3×1 mL) and dried with MgSO₄. The organic layers were pooled, concentrated in vacuo and purified by flash chromatography (2% MeOH-DCM) yielding 0.012 g of **1** (0.022 mmol, 65%). R_f: 0.51, (silica gel, 5% Methanol/DCM); ¹H NMR (400 MHz, MeOD): δ 7.88 (t, $J = 4.8$ Hz, 1H) 7.44-7.06 (m, 15H), 4.27-4.15 (m, 1H), 4.09-3.96 (m, 1H), 3.19-3.08 (m, 2H), 2.72 (qd, $J = 13.4, 6.9$ Hz, 2H), 2.27 (d, $J = 6.6$ Hz, 2H), 2.22-2.05 (m, 2H), 1.85-1.67 (m, 2H), 1.50-1.29 (m, 10H) ppm; ¹³C NMR (100 MHz, MeOD): δ 172.3, 150.2, 138.5, 131.0, 129.6, 127.8, 125.8, 125.1, 120.2, 70.8, 67.3, 43.6, 43.2, 42.5, 38.8, 29.4, 28.6, 27.6, 26.0, 25.8, 23.9, 22.3, 21.8 ppm. ³¹P NMR (121 MHz, CDCl₃): δ 27.03 (tt, $J = 17.4, 12.5$ Hz) ppm. HRMS (ESI) m/z calcd for C₃₀H₃₈NO₆P [M+H]⁺ 540.2438, found 540.2515.

(3*S*,5*R*) Diphenyl (6-(3,5-dihydroxy-6-phenylhexanoylamino)hexyl)phosphonate (**2**)

Compound **10** (0.09 g, 0.20 mmol, 1.3 equiv) was dissolved in HCl/Dioxane (0.5mL, 1.95 mmol, 13 equiv.) and stirred at room temperature under argon. After 1 hour, the solvent was evaporated in vacuo and the free amine **16** was used directly in the next step of the reaction.

Compound *anti*-**15** (0.066g, 0.15 mmol, 1 equiv.) was dissolved in DMF (1.5 mL) and added drop wise to freshly deprotected amine **10**. TBTU (0.058 g, 0.18 mmol, 1.2

equiv.) and DIEA (0.1 mL, 0.45 mmol, 3 equiv.) were added to this solution and the reaction was stirred under argon for 24 hours at room temperature. After checking by TLC for completion, the reaction mixture was poured over brine (10 mL) and extracted with EtOAc (3 × 10 mL). The organic layer was dried with MgSO₄ and concentrated in vacuo. The product was purified by flash column chromatography (20% Acetone/Hexanes) to yield 0.052 g of (3*S*,5*R*) diphenyl (6-(3,5-bis(tert-butyl)dimethylsilyloxy)-6-phenylhexanoylamino)hexylphosphonate (0.068 mmol, 45%). *R*_f: 0.45, (silica gel, 30% Acetone/Hex); ¹H NMR (400 MHz, CDCl₃): δ 7.31-7.12 (m, 15H), 6.33 (br t, *J* = 5.1 Hz, 1H), 4.08-4.02 (m, 1H), 3.90-3.88 (m, 1H), 3.28-3.04 (m, 2H), 2.47-2.28 (m, 2H), 2.06-1.00 (m, 2H), 1.78-1.65 (m, 4H), 1.45-1.28 (m, 8H), 0.82 (s, 9H), 0.81 (s, 9H), 0.00 (s, 6H), -0.03 (s, 3H), -0.18 (s, 3H) ppm; ¹³C NMR (100 MHz, CDCl₃): δ 170.7, 150.4, 138.6, 129.8, 128.2, 126.3, 125.1, 120.5, 71.3, 67.7, 44.4, 44.2, 44.1, 39.1, 30.2, 30.0, 29.3, 26.6, 26.5, 25.9, 25.8, 22.3, 22.3, 18.0, 17.9, -4.5, -4.5, -4.6, -4.7 ppm; ³¹P NMR (121 MHz, CDCl₃): δ 25.68 (tt, *J* = 17.4, 12.5 Hz) ppm; HRMS (ESI) *m/z* calcd for C₄₂H₆₆NO₆PSi₂ [M+Na]⁺ 790.4064, found 790.4021.

(3*S*,5*R*) Diphenyl (6-(3,5-bis(tert-butyl)dimethylsilyloxy)-6-phenylhexanoylamino)hexylphosphonate (0.052 g, 0.068mmol, 1 equiv.) was placed in an Eppendorf tube and dissolved in MeCN (1.7 mL) at room temperature. Pyridine (55 μL, 0.677 mmol, 10 equiv.) and 48 % aqueous HF (285 μL, 6.77 mmol, 100 equiv.) were added to the reaction and the mixture was vortexed for 10 seconds. The reaction proceeded with no stirring for 5 hours. The mixture was then diluted with water (1 mL) extracted with EtOAc (3 × 1 mL) and dried with MgSO₄. The organic layers were pooled, concentrated in vacuo and purified by flash chromatography (2% MeOH-DCM) to yield

0.022 g of **2** (0.041 mmol, 60%). R_f : 0.52, (silica gel, 5% Methanol/DCM); ^1H NMR (400 MHz, MeOD): δ 7.88 (br t, $J = 4.8$ Hz, 1H) 7.37-7.13 (m, 15H), 4.25-4.17 (m, 1H), 4.06-3.98 (m, 1H), 3.17-3.11 (m, 2H), 2.70 (qd, $J = 13.4, 6.9$ Hz, 2H), 2.27 (d, $J = 6.6$ Hz, 2H), 2.22-2.05 (m, 2H), 1.85-1.48 (m, 2H), 1.50-1.29 (m, 10H) ppm; ^{13}C NMR (100 MHz, MeOD): δ 172.5, 150.2, 138.8, 129.6, 129.1, 127.8, 125.7, 125.1, 120.3, 120.2, 68.8, 65.3, 44.2, 43.8, 43.0, 38.7, 29.7, 29.4, 28.6, 25.8, 21.8 ppm; ^{31}P NMR (121 MHz, CDCl_3): δ 25.87 (tt, $J = 17.4, 12.5$ Hz) ppm; HRMS (ESI) m/z calcd for $\text{C}_{30}\text{H}_{38}\text{NO}_6\text{P}$ $[\text{M}+\text{Na}]^+$ 62.2337, found 62.2341.

2.5.3 Kinetic analysis of hydrolysis by DEBS TE

TE-catalyzed hydrolysis of thioester substrates were monitored by the formation of 5-thio-2-nitrobenzoate by the reaction of TE-hydrolyzed N-acetylcysteamine with 5,5'-dithiobis-2-nitrobenzoic acid (dTNB). A typical kinetic assay mixture consisted of 2.5 μM inhibited DEBS TE, 50 mM phosphate buffer (pH 7.38), 4 % (v/v) saturated dTNB in water, 5 mM substrate (100 mM stock solution in DMSO), and 10 % (v/v) DMSO in a total volume reaction of 200 μL .

The formation of the free thiol was quantified by measuring the absorption at 412 nm using a Thermo Scientific Evolution 300 UV-Vis spectrophotometer. The reactions were performed at room temperature and were absorption was measured at 5, 10, 15, 20, 25, 30, 45 and 60 minutes. Initial velocities were determined by linear regression analysis and compared to the reaction with an uninhibited sample of DEBS TE.

Cloning, overexpression and purification of a new construct of DEBS TE

The gene sequence encoding the TE domain of DEBS was amplified by PCR from the plasmid pRSG33 REF DNA using primers DTe_F5'-

TATTAACCATGGGCAGCAGCGCTCTTCGCGAC-3' and DTe_R5'-

AATTAACTCGAGTTACGAATTCCTCCGCCAGCC-3', digested with NcoI and

XhoI restriction enzymes and cloned into these sites in the pJ411 (DNA 2.0) -derived

expression vector pBacP to yield pBacP_TeC. A deletion of the sequence for four amino acid residues was achieved using site-directed mutagenesis with primers 5'-

GCAGCGAGAATTTGTACTIONTCCAAAGCAGCGCTCTT-3' and 5'-

AAGAGCGCTGCTTTGGAAGTACAAATTCTCGCTGC-3' to yield pBacP_TeX.

Protein expression from pBacP_TeX was performed in *Escherichia coli* BL21 (DE3)

cells. Cells were grown at 37 °C in lysogeny broth (LB) supplemented with kanamycin (30 µg/ml) until an optical density at 600 nm (OD_{600nm}) of 0.6. The culture was then

cooled to 30 °C, expression was induced with 1 mM isopropyl 1-thio-β-D-

galactopyranoside, and the culture was allowed to grow for 5 hours at 30 °C. Cells were

harvested by centrifugation (4,000 × g for 20 minutes), resuspended in lysis buffer (100

mM Tris-HCl, 100 mM NaCl, 10 mM imidazole, pH 7.5) and lysed by four cycles of cell

disruption with an EmulsiFlex-C3 apparatus (Avestin) at a pressure of 13,000 pounds per

square inch. Cellular debris was removed by centrifugation at 15,000 × g for 45 minutes,

and the supernatant was loaded into a 5 mL Ni²⁺-bound HiTrap Fast Flow column (GE

Healthcare) connected to an ÄKTA purifier (GE Healthcare). The column was

extensively washed with the wash buffer (100 mM Tris-HCl, 100 mM NaCl, 15 mM

imidazole, pH 7.5) and then eluted with a linear gradient of imidazole up to 300 mM.

Fractions containing high concentrations of TE protein were identified by SDS-PAGE, pooled and dialysed using a 10 kDa cutoff membrane at 20 °C overnight, against 2 liters of digestion buffer (20 mM Tris/HCl, 100 mM NaCl, 3 mM β -mercaptoethanol (β ME), 0.5 mM EDTA, pH 8.0) with concurrent incubation with 1 mg tobacco etch virus (TEV) protease per 40 mg of protein sample to cleave the His₆tag. The impurities and remaining tagged protein were removed by reapplying the sample to the Ni²⁺-column equilibrated in wash buffer. The flow through was diluted 10 times in a buffer of 100 mM Tris/HCl, 10 mM NaCl, pH 7.5 and loaded onto a HiTrap Q sepharose Fast Flow column (GE Healthcare). Protein was eluted with a linear gradient of sodium chloride (10 mM - 1 M) in 100 mM Tris-HCl, pH7.5. The purified protein fractions were pooled, concentrated to 5 mg/mL and applied to a HiLoad 16/60 Superdex 75 (GE Healthcare) equilibrated and run in 20 mM Tris-HCl, 100 mM NaCl, 2 mM DTT, pH 7.5. Finally, purified protein was concentrated to 5 or 10 mg/mL and used immediately or flash frozen in liquid nitrogen and stored at -80 °C. A yield of ~50 mg purified TE was obtained per liter of culture. Protein concentration was determined by measuring OD_{280nm} and using an extinction coefficient of 43555 M⁻¹ cm⁻¹.

Activity and inhibition assays

Activity of TE₁₅₋₂₈₃ was measured using Ellman's assay.[43] Assays were of 600 μ L volume with 50 mM KH₂PO₄/K₂HPO₄ pH 7.4, 0.2 mM 5,5'-dithiobis-(2-nitrobenzoic acid) (DTNB), 0.5 mM substrate **4**, 10 % DMSO and 5 μ M protein. Reactions proceeded at room temperature for 20 minutes and were monitored by optical absorbance at 412 nm using a UV-Vis spectrophotometer (DU 730 Beckman Coulter).

Inhibition with the diphenyl allylphosphonate inhibitor was performed by incubating 5 μM TE overnight at room temperature with 35 μM diphenyl allylphosphonate in 50 mM $\text{KH}_2\text{PO}_4/\text{K}_2\text{HPO}_4$ pH 7.4, 10% DMSO. Inhibition with diphenyl phosphonates **1** and **2** was performed by incubating 5 μM TE overnight at 37 °C with 54 μM diphenyl phosphonate, 50 mM $\text{KH}_2\text{PO}_4/\text{K}_2\text{HPO}_4$ pH 7.4 and 10% DMSO. Activity of inhibited protein was measured as described above.

Crystallography

Crystals of TE were obtained at 20 °C by using the sitting-drop vapor-diffusion method with a 1:1 (v/v) ratio of protein (5 or 10 mg/mL in 20 mM Tris-HCl, 100 mM NaCl, 2 mM DTT, pH 7.5) to precipitation solution (100 mM Na-cacodylate, 35-38% polyethylene glycol (PEG) 300, 0.18-0.24 M Ca-acetate, pH 6.5). Soaking experiments were performed by incubating crystals with 3.6 mM diphenyl allylphosphonate at 20 °C for 48 hours or 5 mM **1** and **2** at 20 °C for 2 weeks in 10% DMSO. For co-crystallization of TE with **1** and **2**, the complexes were formed by incubating 50 μM TE with 5.4 mM diphenyl phosphonate, 50 mM $\text{KH}_2\text{PO}_4/\text{K}_2\text{HPO}_4$ pH 7.4 and 10% DMSO overnight at 30 °C and re-purified by gel filtration with a Superdex S75 10/300 GL column in 20 mM Tris-HCl, 100 mM NaCl, 2 mM DTT, pH 7.5. The resulting complexes were crystallized using the same protocol for the unliganded protein.

Crystals were directly flash-cooled in a stream of nitrogen gas. Diffraction data were collected at 100 K source using a Rigaku MicroMax-007 HF and 1.54 Å radiation under a

nitrogen stream at the McGill Center for Structural Biology or on the beamline 8 at Canadian Light Source (CLS, Saskatoon, Canada). Diffracted intensities were processed using both the CCP4 package (MOSFLM and SCALA) and HKL2000. An initial model was obtained using the molecular replacement program PHASER[44] with the crystal structure of the TE domain of DEBS (PDBID: 1KEZ) as a search model. Refinement was carried out with REFMAC5 and model building was performed using COOT. All structures were validated using PROCHECK and COOT validation tools. Atomic coordinates and restraints of ligands used for the structures of the different complexes were generated with the PRODRG2 server (<http://davapc1.bioch.dundee.ac.uk/prodrg/>) and JLigand 0.1 beta. Figures were prepared with the program PyMOL (Schrödinger). Atomic coordinates have been deposited at the protein database under accession codes: 5D3K and 5D3Z. Crystal parameters, space groups, data collection and refinement statistics are given in Table 1.

Mass spectrometry analysis of TE-inhibitor complexes

TE₁₅₋₂₈₃ (50 μ M) was incubated overnight at 30 °C with 5.4 mM *syn* diphenyl phosphonate **1** or with 3.6 mM diphenyl allylphosphonate in 50 mM KH₂PO₄/K₂HPO₄ pH 7.4 and 10 % DMSO. Excess inhibitor was removed and the resulting complex was transferred into a solution that was identical to crystallization solution except that it contained 20% PEG300, using 10 kDa molecular weight cut-off spin filters. Complexes were incubated at room temperature for 1 day, 7 days and 1 month before LC-MS analysis. LC-MS was performed stepwise by LC with an Agilent Eclipse XDB-C8 reverse phase column (4.6 \times 150 mm, 5 μ m) and a 10 minute gradient from 0.1% TFA in

H₂O to 0.1% TFA in acetonitrile at 0.75 mL/min, and then direct injection onto a ESI-MS (Esquire HCT Ultra; Bruker Daltonics) using an ESI nebulizer and syringe pump set to infuse at 240 μ L/hr. Mass spectra were acquired in positive mode over a mass range of 800-2800 m/z for an average of 5 min. Acquired spectra were averaged and the charge states were assigned using a charge state ruler (Esquire Data Analysis; Bruker Daltonics).

Acknowledgements

This work was supported by funding from Natural Sciences and Engineering Research Council of Canada, Canadian Foundation for Innovation and the University of Ottawa to C. N. B., by CHIR grant 106615 and a Canada Research Chair in Macromolecular Machines to T.M.S. and by an NSERC Alexander Graham Bell studentship to J. R. We thank Diego Alonzo for the processing of kinetic data.

Table 1. Crystallographic statistics for unliganded DEBS TE₁₅₋₂₈₃ and the complex with allylphosphonate

Data set	Apo	Allylphosphonate complex
Data collection		
Space group	P 3 2 1	P 3 2 1
Unit cell dimensions <i>a, b, c</i> (Å)	112.92, 112.92, 42.97	112.54, 112.54, 42.78
Resolution limits (Å)	36.96-1.7 (1.79-1.7)	32.15-2.1 (2.14-2.1)
No. of measured reflections	140978 (20318)	194129 (11668)
No. of unique reflections	34552 (5064)	18454 (1444)
Completeness (%)	99.1 (100.0)	99.6 (98.2)
R_{sym}	0.12 (0.47)	0.12 (0.29)
$\langle I / \sigma \rangle$	7.3 (2.8)	20.5 (6.3)
B_{Wilson} (Å ²)	14.5	17.0
Refinement statistics		

Resolution range	36.96-1.7	32.15-2.1
No. of reflections work/test	32914/1638	17518/932
No. of molecules /A.U	1	1
R_{work} (%)	15.6	16.9
R_{free} (%)	18.7	19.0
No. of atoms		
Protein atoms	2018	1982
Ligand atoms	-	4
Water/other solvent heteroatoms	258	227
<hr/>		
r.m.s.d. ^b bond lengths (Å)	0.021	0.007
r.m.s.d. bond angles (°)	1.995	1.14
Mean temperature factor (Å ²)	17	18
Ramachandran Plot (%)		
Favoured	98	98
Allowed	2	2
Outliers	-	-

^a Values in parentheses are for the highest resolution shell

^b r.m.s.d. root mean square deviation

References

- [1] K.J. Weissman, R. Müller, Protein-protein interactions in multienzyme megasynthetases, *Chembiochem*, 9 (2008) 826–48.
- [2] W. Xu, K. Qiao, Y. Tang, Structural analysis of protein-protein interactions in type I polyketide synthases, *Crit. Rev. Biochem. Mol. Biol.*, 48 98–122.
- [3] D. Portevin, C. De Sousa-D’Auria, C. Houssin, C. Grimaldi, M. Chami, M. Daffé, C. Guilhot, A polyketide synthase catalyzes the last condensation step of mycolic acid biosynthesis in mycobacteria and related organisms, *Proc. Natl. Acad. Sci. U. S. A.*, 101 (2004) 314–9.

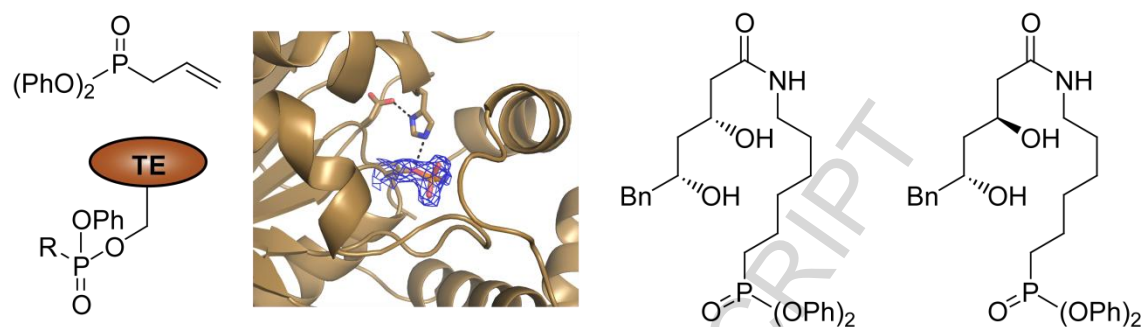
- [4] L.R. Camacho, D. Ensergueix, E. Perez, B. Gicquel, C. Guilhot, Identification of a virulence gene cluster of *Mycobacterium tuberculosis* by signature-tagged transposon mutagenesis, *Mol. Microbiol.*, 34 (1999) 257–67.
- [5] K.M. George, D. Chatterjee, G. Gunawardana, D. Welty, J. Hayman, R. Lee, P.L. Small, Mycolactone: a polyketide toxin from *Mycobacterium ulcerans* required for virulence, *Science*, 283 (1999) 854–7.
- [6] C.T. Walsh, The chemical versatility of natural-product assembly lines, *Acc. Chem. Res.*, 41 (2008) 4–10.
- [7] F. Kopp, M.A. Marahiel, Macrocyclization strategies in polyketide and nonribosomal peptide biosynthesis, *Nat. Prod. Rep.*, 24 (2007) 735–49.
- [8] L. Du, L. Lou, PKS and NRPS release mechanisms, *Nat. Prod. Rep.*, 27 (2010) 255–78.
- [9] M. Nardini, B.W. Dijkstra, Alpha/beta hydrolase fold enzymes: the family keeps growing, *Curr. Opin. Struct. Biol.*, 9 (1999) 732–7.
- [10] M.E. Horsman, T.P.A. Hari, C.N. Boddy, Polyketide synthase and non-ribosomal peptide synthetase thioesterase selectivity: logic gate or a victim of fate?, *Nat. Prod. Rep.*, (2015).
- [11] C.M. Kao, G. Luo, L. Katz, D.E. Cane, C. Khosla, Manipulation of macrolide ring size by directed mutagenesis of a modular polyketide synthase, *J. Am. Chem. Soc.*, 117 (1995) 9105–9106.
- [12] C.M. Kao, G. Luo, L. Katz, D.E. Cane, C. Khosla, Engineered Biosynthesis of Structurally Diverse Tetraketides by a Trimodular Polyketide Synthase, *J. Am. Chem. Soc.*, 118 (1996) 9184–9185.
- [13] J.R. Jacobsen, C.R. Hutchinson, D.E. Cane, C. Khosla, Precursor-directed biosynthesis of erythromycin analogs by an engineered polyketide synthase, *Science*, 277 (1997) 367–9.
- [14] C.M. Kao, M. McPherson, R.N. McDaniel, H. Fu, D.E. Cane, C. Khosla, Gain of Function Mutagenesis of the Erythromycin Polyketide Synthase 2 Engineered Biosynthesis of an Eight-Membered Ring Tetraketide Lactone, *J. Am. Chem. Soc.*, 119 (1997) 11339–11340.
- [15] R.S. Gokhale, D. Hunziker, D.E. Cane, C. Khosla, Mechanism and specificity of the terminal thioesterase domain from the erythromycin polyketide synthase, *Chem. Biol.*, 6 (1999) 117–25.

- [16] W. He, J. Wu, C. Khosla, D.E. Cane, Macrolactonization to 10-deoxymethynolide catalyzed by the recombinant thioesterase of the picromycin/methymycin polyketide synthase, *Bioorg. Med. Chem. Lett.*, 16 (2006) 391–4.
- [17] A. Pinto, M. Wang, M. Horsman, C.N. Boddy, 6-Deoxyerythronolide B synthase thioesterase-catalyzed macrocyclization is highly stereoselective, *Org. Lett.*, 14 (2012) 2278–81.
- [18] T.P.A. Hari, P. Labana, M. Boileau, C.N. Boddy, An evolutionary model encompassing substrate specificity and reactivity of type I polyketide synthase thioesterases, *Chembiochem*, 15 (2014) 2656–61.
- [19] S.C. Tsai, L.J. Miercke, J. Krucinski, R. Gokhale, J.C. Chen, P.G. Foster, D.E. Cane, C. Khosla, R.M. Stroud, Crystal structure of the macrocycle-forming thioesterase domain of the erythromycin polyketide synthase: versatility from a unique substrate channel, *Proc. Natl. Acad. Sci. U. S. A.*, 98 (2001) 14808–13.
- [20] S.-C. Tsai, H. Lu, D.E. Cane, C. Khosla, R.M. Stroud, Insights into channel architecture and substrate specificity from crystal structures of two macrocycle-forming thioesterases of modular polyketide synthases, *Biochemistry*, 41 (2002) 12598–606.
- [21] M. Wang, C.N. Boddy, Examining the role of hydrogen bonding interactions in the substrate specificity for the loading step of polyketide synthase thioesterase domains, *Biochemistry*, 47 (2008) 11793–803.
- [22] D.L. Akey, J.D. Kittendorf, J.W. Giraldes, R.A. Fecik, D.H. Sherman, J.L. Smith, Structural basis for macrolactonization by the pikromycin thioesterase, *Nat. Chem. Biol.*, 2 (2006) 537–42.
- [23] J.W. Giraldes, D.L. Akey, J.D. Kittendorf, D.H. Sherman, J.L. Smith, R.A. Fecik, Structural and mechanistic insights into polyketide macrolactonization from polyketide-based affinity labels, *Nat. Chem. Biol.*, 2 (2006) 531–6.
- [24] A.M. Lambeir, M. Borloo, I. De Meester, A. Belyaev, K. Augustyns, D. Hendriks, S. Scharpé, A. Haemers, Dipeptide-derived diphenyl phosphonate esters: mechanism-based inhibitors of dipeptidyl peptidase IV, *Biochim. Biophys. Acta*, 1290 (1996) 76–82.
- [25] B.F. Gilmore, J.F. Lynas, C.J. Scott, C. McGoohan, L. Martin, B. Walker, Dipeptide proline diphenyl phosphonates are potent, irreversible inhibitors of seprase (FAPalpha), *Biochem. Biophys. Res. Commun.*, 346 (2006) 436–46.
- [26] R.J. Cohen, D.L. Fox, J.F. Eubank, R.N. Salvatore, Mild and efficient Cs₂CO₃-promoted synthesis of phosphonates, *Tetrahedron Lett.*, 44 (2003) 8617–8621.

- [27] H. Sun, W.R. Roush, D. Hughes, Synthesis OF (+)-B-allyldiisopinocampheylborane and its reaction with aldehydes, *Organic Synth.*, 88 (2011) 87–102.
- [28] E.N. Jacobsen, I. Marko, W.S. Mungall, G. Schroeder, K.B. Sharpless, Asymmetric dihydroxylation via ligand-accelerated catalysis, *J. Am. Chem. Soc.*, 110 (1988) 1968–1970.
- [29] H.C. Brown, P.K. Jadhav, Asymmetric carbon-carbon bond formation via .beta-allyldiisopinocampheylborane Simple synthesis of secondary homoallylic alcohols with excellent enantiomeric purities, *J. Am. Chem. Soc.*, 105 (1983) 2092–2093.
- [30] B.S. Bal, W.E. Childers, H.W. Pinnick, Oxidation of α,β -un saturated aldehydes, *Tetrahedron*, 37 (1981) 2091–2096.
- [31] J. Oleksyszyn, J.C. Powers, Amino acid and peptide phosphonate derivatives as specific inhibitors of serine peptidases, *Methods Enzymol.*, 244 (1994) 423–41.
- [32] M.L. Bender, F.C. Wedler, Phosphate and carbonate ester “aging” reactions with -chymotrypsin Kinetics and mechanism, *J. Am. Chem. Soc.*, 94 (1972) 2101–9.
- [33] J.A. Bertrand, J. Oleksyszyn, C.M. Kam, B. Boduszek, S. Presnell, R.R. Plaskon, F.L. Suddath, J.C. Powers, L.D. Williams, Inhibition of trypsin and thrombin by amino(4-amidinophenyl)methanephosphonate diphenyl ester derivatives: X-ray structures and molecular models, *Biochemistry*, 35 (1996) 3147–55.
- [34] E.F. Jansen, F. Nutting, Inhibition of the proteinase and esterase activities of trypsin and chymotrypsin by diisopropyl fluorophosphate; crystallization of inhibited chymotrypsin, *J. Biol. Chem.*, 179 (1949) 189–99.
- [35] E.F. Jansen, F. Nutting, A.K. Balls, Mode of inhibition of chymotrypsin by diisopropyl fluorophosphate; introduction of phosphorus, *J. Biol. Chem.*, 179 (1949) 201–4.
- [36] E.F. Jansen, F. Nutting, R. Jang, A.K. Balls, Mode of inhibition of chymotrypsin by diisopropyl fluorophosphate II Introduction of isopropyl and elimination of fluorine as hydrogen fluoride, *J. Biol. Chem.*, 185 (1950) 209–20.
- [37] H. Zhang, R. Tsukuhara, G. Tigyi, G.D. Prestwich, Synthesis of cyclic phosphonate analogues of (lyso)phosphatidic acid using a ring-closing metathesis reaction, *J. Org. Chem.*, 71 (2006) 6061–6.
- [38] L. Gavara, C. Petit, J.-L. Montchamp, DBU-promoted alkylation of alkyl phosphinates and H-phosphonates, *Tetrahedron Lett.*, 53 (2012) 5000–5003.

- [39] G. Baccolini, C. Boga, One-pot synthesis of unsymmetrical aryl methylphosphinates by insertion of dichlorophosphines into the OMe bond of anisoles, *Tetrahedron Lett.*, 42 (2001) 6121–6124.
- [40] A. Holý, Simple Method for Cleavage of Phosphonic Acid Diesters to Monoesters, *Synthesis (Stuttg.)*, 1998 (1998) 381–385.
- [41] O. Demmer, A.O. Frank, F. Hagn, M. Schottelius, L. Marinelli, S. Cosconati, R. Brack-Werner, S. Kremb, H.-J. Wester, H. Kessler, A conformationally frozen peptoid boosts CXCR4 affinity and anti-HIV activity, *Angew. Chem. Int. Ed. Engl.*, 51 (2012) 8110–3.
- [42] M.S. Egbertson, C.T.-C. Chang, M.E. Duggan, R.J. Gould, W. Halczenko, G.D. Hartman, W.L. Laswell, J.J. Lynch, R.J. Lynch, Non-Peptide Fibrinogen Receptor Antagonists 2 Optimization of a Tyrosine Template as a Mimic for Arg-Gly-Asp, *J. Med. Chem.*, 37 (1994) 2537–2551.
- [43] G.L. Ellman, Tissue sulfhydryl groups, *Arch. Biochem. Biophys.*, 82 (1959) 70–7.
- [44] A.J. McCoy, R.W. Grosse-Kunstleve, P.D. Adams, M.D. Winn, L.C. Storoni, R.J. Read, Phaser crystallographic software, *J. Appl. Crystallogr.*, 40 (2007) 658–674.

Graphical abstract



Highlights

- 1.7 Å resolution structure of a new construct of the erythromycin thioesterase
- diphenyl phosphonate inhibitors of the erythromycin thioesterases were synthesized and assayed
- 2.1 Å resolution structure of allylphosphonate adduct of the erythromycin thioesterase
- Slow maturation of initial phosphonate-enzyme adduct limits use of diphenyl phosphonates esters